INTERFACE LAYER MODIFICATIONS USING POLYELECTROLYTES FOR HIGH EFFICIENCY ORGANIC SOLAR CELL

A DISSERTATION SUBMITTED TOWARDS THE PARTIAL FULFILLMENT OF THE REQUIREMENT FOR THE AWARD OF DEGREE OF

MASTER OF TECHNOLOGY

IN

NANOSCIENCE AND TECHNOLOGY

SUBMITTED BY

SRIRAJ PILLAI

(ROLL NO. 2K11/NST/16)

UNDER THE SUPERVISION OF

Dr. SURESH CHAND — **(Chief Scientist, NPL, Delhi)**

Dr. J.P. TIWARI — **(Scientist, NPL, Delhi)**

Dr. PAWAN KUMAR TYAGI

(Asst. Professor, DTU, Delhi)

DEPARTMENT OF APPLIED PHYSICS

DELHI TECHNOLOGICAL UNIVERSITY, BAWANA ROAD, DELHI-110042

JULY-2013

CERTIFICATE-II

This is to certify that **Mr. Sriraj Pillai** (2K11/NST/16) has carried out the major project titled "**Interface Layer Modifications Using Polyelectrolytes for High Efficiency Organic Solar Cell**" as a partial requirement for the award of Master of Technology degree in Nanoscience and Technology by Delhi Technological University, Delhi. This work was carried out in National Physical Laboratory, New Delhi. The matter contained in this report has not been submitted elsewhere for the award of any other degree.

Prof. S.C. Sharma
HOD, Dept. of Applied Physics
Delhi Technological University
Delhi-110042

Place:
Date:

Dr. Pawan K. Tyagi
Assistant Professor
Delhi Technological University
Delhi-110042

Place:
Date:

DECLARATION BY THE CANDIDATE

I hereby declare that the work presented in this dissertation entitled "**Interface Layer Modifications using Polyelectrolytes for High Efficiency Organic Solar Cell**" has been carried out by me under the guidance of external supervisors Dr. Suresh Chand and Dr. J.P Tiwari, National Physical Laboratory and internal supervisor Dr. Pawan Kumar Tyagi, Assistant Professor, Department of Applied Physics, Delhi Technological University, Delhi and is hereby submitted for the partial fulfillment for the award of degree of Master of Technology in Nanoscience and Technology at Applied Physics Department, Delhi Technological University, Delhi.

I further undertake that the work embodied in this major project has not been submitted for the award of any other degree elsewhere.

Sriraj Pillai

Roll no.- 2K11/NST/16

M.Tech

(Nanoscience and Tech.)

Delhi Technological University

ACKNOWLEDGEMENT

I express my deep sense of gratitude to **Dr. Suresh Chand** who was my supervisor for providing me an opportunity to work in Organic and Hybrid Solar Cell Section, NPL. His wide knowledge, logical way of thinking and pitch-perfect instincts on all matters large and small have been of great value to me. I want to express my deep sense of gratitude to my supervisor **Dr. J.P. Tiwari** who was my co-guide in NPL. His constructive criticism and insight was necessary without which the project would not have shaped as it has.

I express my gratitude to **Prof. S.C. Sharma**, Head of Department, Department of Applied Physics, Delhi Technological University, Delhi and **Dr. Pawan Kumar Tyagi** who was my guide and branch coordinator. Their invaluable support and encouragement was very vital towards completing this thesis.

I would like to acknowledge all members of Organic and Hybrid Solar Cell Section at NPL for their kind support in my work, with very special thanks to senior research fellow **Mr. Abhishek Sharma, Dr. Farman Ali** and **Mr. Neeraj Chaudhary** for their everlasting support and efforts. I further thank **Dr. G.D. Sharma** and **Mr. Ramil Kumar Bhardwaj**. Words cannot express my gratefulness to them for providing their valuable help and time whenever required.

I also want to thank my classmates at Delhi Technological University, Delhi and in particular **Ms. Prashansa Dalal** and **Ms. Sonal Parakh**. I never could have guessed that research could be this fun with you two around.

I take pride of myself being the son of ideal parents for their everlasting desire, sacrifice, affectionate blessings, and help, without which it would not have been possible for me to complete my studies.

Last but not the least my loving grandparents have been very keen on my completing this work. Their encouragement and blessings made it possible for me to achieve this.

Sriraj Pillai

Roll No.- 2K11/NST/16

M.Tech (Nanoscience and Tech.)

E-mail: srirajpillai@gmail.com

Table of Contents

List of Figures and Tables

List of Abbreviations

1. **BHJ** - Bulk Heterojunction
2. **DEA** - Diethanolamine
3. **DSSC** - Dye Synthesized Solar Cell
4. **ETL** - Electron Transport Layer
5. **FF** - Fill Factor
6. **HOMO** - Highest Occupied Molecular Orbital
7. **HTL** - Hole Transport Layer
8. **ITO** - Indium Tin Oxide
9. **LUMO** -Lowest Unoccupied Molecular Orbital
10. **OSC** - Organic Solar Cell
11. **OPV** - Organic Photovoltaic
12. **PCE** - Power Conversion Effeciency
13. **PCBM** - [6,6]- $C_{61or\ 71}$-Butyric acid Methyl ester
14. **PCDTBT** - Poly[[9-(1-octylnonyl)-9H-carbazole-2,7-diyl]-2,5-thiophenediyl-2,1,3-benzothiadiazole-4,7-diyl-2,5-thiophenediyl]
15. **PDADMAC** - Poly(diallyldimythylammonium chloride)
16. **PEDOT:PSS** - poly(3,4-ethylenedioxythiophene):poly(styrenesulfonate)
17. **PSS** - Poly(4-styrenesulfonic acid)
18. **P3HT** - poly (3-hexylthiophene)

Abstract

Considering the present world energy consumption and the exponential growth in human population, the growing energy need has to be mollified by the use of renewable sources of energy such as solar energy. Development is necessary but not at the cost of the future generations. The need of the hour is sustainable development. Thus, concerns about global warming and diminishing fossil fuel reserves have accelerated the search for low cost sources of renewable energy. Organic photovoltaics (OPVs) could be one such source. The investigation in this thesis takes a step in this direction.

The solar cells investigated in this thesis are BHJ solar cells. Fabrication of such cells involve etching of the substrates, preparation of the active material and buffer layer solutions, cleaning of the substrates, coating and deposition of the materials over the substrate. Finally once these solar cells are fabricated, J-V characterization of these cells are carried out to determine the device parameters- power conversion efficiency (PCE), open circuit voltage (V_{OC}), fill factor (FF) and short circuit current density (J_{SC}).

In this thesis we have focused on the interface layers in conventional and inverted organic solar cells. In case of conventional devices, we have tried to replace PEDOT:PSS by MoO_3 layer and whereas in case of inverted devices, we have applied a polyelectrolyte based approach for modifying the ZnO interface layer.

Herein, we have used solution based approach for MoO_3 and demonstrated that PEDOT:PSS can be successfully replaced by solution processed MoO_3. For the modification of interface layer in case of inverted devices we have used the combination of zinc oxide and polyelectrolyte viz. ZnO-PDADMAC and ZnO-PSS nanocomposite. Both of these combinations have shown remarkable increase in the device parameters such as- J_{SC} and η. However, the Zno-PDADMAC nanocomposite has shown a huge increase of ~ 22 times in device efficiency. These results have been discussed in detail in this thesis.

Keywords: Polyelectrolyte, Zinc Oxide, Solution Process MoO_3, Bulk Heterojunction, Organic Solar Cell

Chapter 1

Introduction

1.1 Need for Solar Energy

Energy is a precious resource for humans from centuries. With the exponential increase in human population the energy demands have increased tremendously and there is no way that we can meet the needs of every human being on earth by solely relying on fossil fuels which unfortunately is the current trend. Moreover, fossil fuels are a non-renewable resource that once depleted would take millions of years to regenerate. With the current consumption we are heading towards this disaster at a much faster rate. We need to find other alternatives to meet the increasing energy demands. Figure 1.1 shows the current and the predicted world energy consumption.

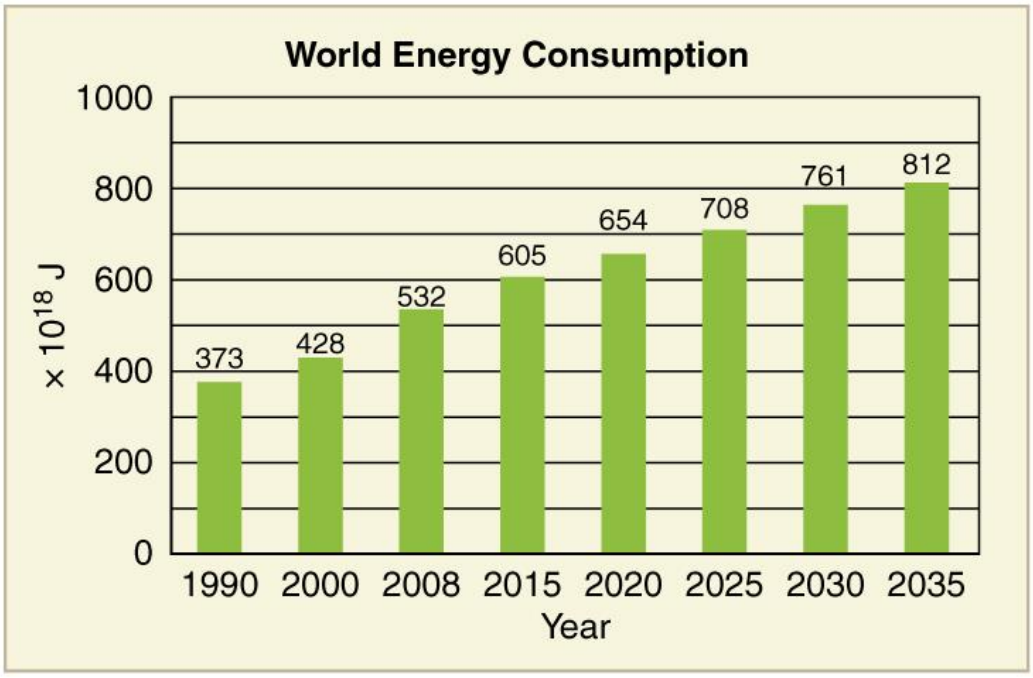

Figure 1.1 World energy consumption [1]

Another consequence of using fossil fuels is the emission of greenhouse gases. The primary greenhouse gases (GHGs) present in the earth's atmosphere are water vapour, carbon dioxide, methane, nitrous oxide and ozone. These gases trap heat in the atmosphere thus leading to global warming and unwanted climate changes. The burning

of fossil fuels has contributed to 40% rise in the concentration of carbon dioxide in the atmosphere from 280 ppm to 400 ppm [2]. Anthropogenic carbon dioxide (CO_2 released due to human activities) come from the combustion of carbon based fuels such as coal, wood, oil and natural gas.

In today's world the demand for fossil fuels as described earlier is increasing in proportion to the world population. Development is important but not at the cost of destroying the very world we live in. In a report produced by the Intergovernmental Panel on Climate Change, a panel assembled by the United Nations in 2007, the threat due to greenhouse gases were outlined (GHGs). The anthropogenic greenhouse gas emission along with the global rise in energy demands are one of the pressing issues we face today. These issues need to be resolved at the earliest in order to ensure a bright future for our future generations. Thus, the need of the hour is sustainable development.

The need for sustainable development has accelerated research in the areas of renewable sources of energy such as- solar energy. When it comes to renewable sources of energy, solar energy easily takes the lead. Incoming solar radiation intensity is around 1000 W/m^2 indicating that roughly 1.5 X 10^7 W hits the earth's surface. This is over 500 times the global demand for power. This shows that undoubtedly solar power is going to be one of the prime sources of energy in the coming decades.

Thus, the need of the hour is to avoid the over exploitation of these fossil fuels and to rely on renewable sources of energy such as solar energy, wind energy and hydroelectricity to fulfil the energy demands of the coming generations. Solar energy is by far the renewable energy source with the greatest potential (Table 1.1). Here, our focus is on solar energy.

Table 1.1 Energy available for harvesting from different sources compared to the global energy demand [3]

Global consumption	**Hydro**	**Geothermal**	**Wind**	**Solar**
15 TW	7. 2 TW	32 TW	870 TW	86,000 TW

1.2 Basics of a Solar Cell Device

Solar cell as we know is a semiconducting device. It converts solar energy into electrical energy (photovoltaic effect). Light which is made up of packets of energy, called photons, its energy depends on the frequency, or colour, of the light. The solar spectrum covers ultra violet to infrared wavelength ranges. Only 30% of incident light energy is in the visible light range, while over 50% is in the infrared range (Figure 1.2).

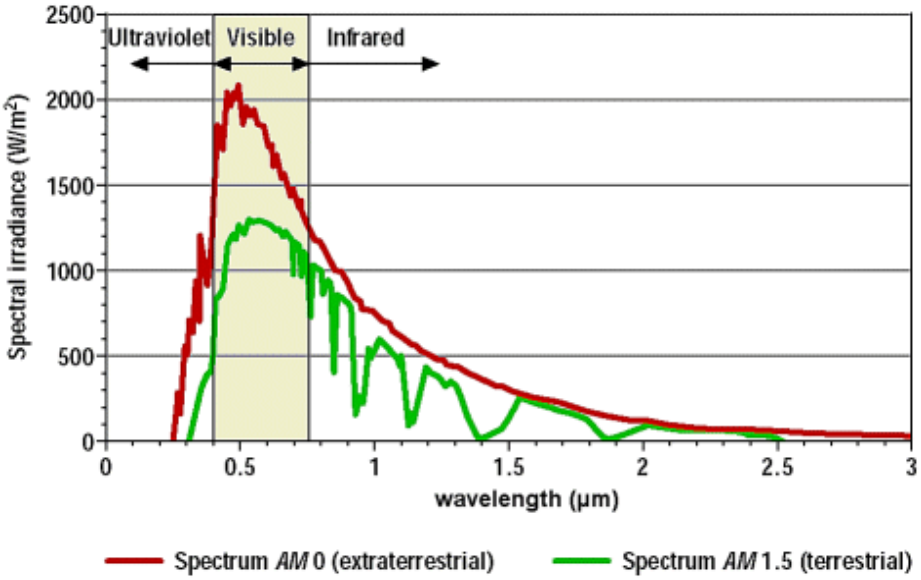

Figure 1.2 Solar Radiation Spectrum

The photons in UV and visible range have enough energy to pump electrons in semiconducting material, and this can be effectively used for charge generation. However, IR waves are too weak to generate electricity using conventional PV technology.

1.3 Generations of Solar Cells

Solar cells can be best classified in terms of generations i.e. the development and variations in solar cells with time.

So far there have been three such generations of solar cells as follows:

1.3.1 First Generation:-

Single PN junction silicon solar cells come under first generation PVs. This category of solar cells is the most commercialised one covering 90% of the photovoltaic market. [4]

The most important parameter of the performance of a solar cell is its Power conversion efficiency (PCE), i.e. the percentage of incoming solar radiation that is converted to usable power by the solar cell. So far, the highest theoretical efficiency that is reported by Shockley and Queissier i.e. 33% for any type of single cell solar cell with a band gap of 1.1 eV [5]. Kerr et al. calculated that for a 90μm thick single junction solar cell to be 29% [6].

(a) Monocrystalline Silicon Cells:-

Solar cells made from thin wafers of silicon are the most prominent solar cell technology currently in spite of being the oldest. These cells are sliced from large single crystals that have been grown in a controlled environment with tremendous efforts and hence called as monocrystalline solar cells. A panel is made up of a number of cells laid out in a grid and are a few inches across (Figure 1.3).

They have a higher efficiency (up to 24.2%) as compared to other types of cells which means that more electricity can be produced from a given panel area [7].

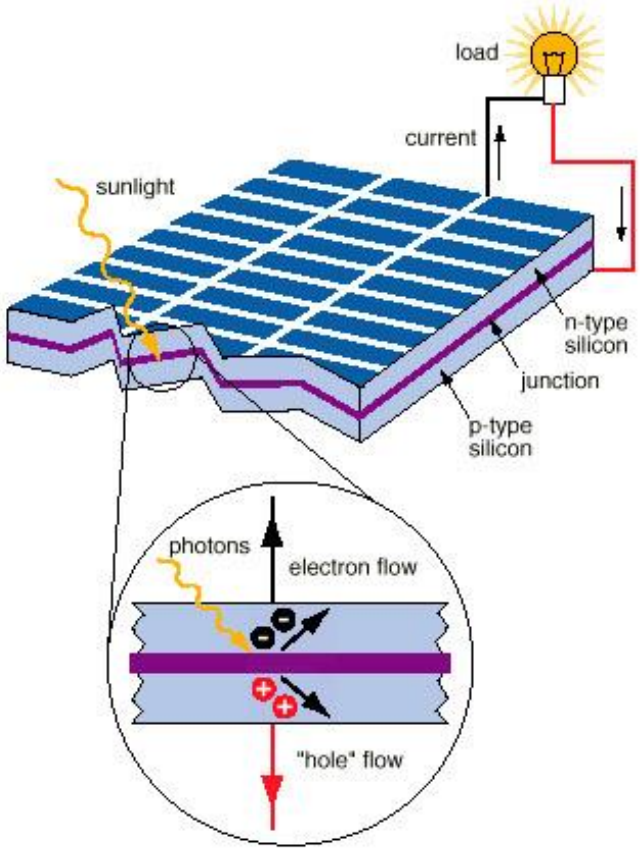

Figure 1.3 A basic schematic diagram for first generation solar cells.

(b) Polycrstalline Silicon Cells-

The production of silicon wafers in moulds from multiple silicon crystals rather than from a single crystal is obviously cheaper and easier as compared to the production of monocrystalline solar cells, as the growing environment need not be as controlled and specific. A number of silicon crystals are grown together to make polycrystalline solar cells. No doubt panels on these cells are cheaper per unit area but they suffer in efficiency (up to 19.3%).

(c) Amorphous Silicon Cells-

In amorphous silicon cells of silicon crystals are not grown as is done in the previous two types, instead silicon is deposited in a very sleek layer on a backing substrate such as metal, glass, or plastic. In these cells various silicon layers are mixed with impurities accordingly to respond to various wavelengths of light and are laid in a stack to improve efficiency.

d) Hybrid Silicon Cells-

As the name suggests the origin of this type of silicon solar cells was after exploring ways of combining different materials to make a hybrid with better efficiency, stability at reduced costs.

Recently introduced hybrid HIT cell consisted of a layer of amorphous silicon over single crystal wafers. It was found that the efficiency improved and even stabilised with fluctuations in temperature of the place.

First generation solar cells have highest efficiencies and lifetimes among all other types. The only limitation it faces is its high production cost that prevents them from being economically competitive and hence open doors for other research domains. In August 2010, Solar buzz, an international solar energy research and consulting firm, confirmed the residential price per kilowatt-hour of solar electricity was approximately 35 cents [8].

1.3.2 Second Generation:-

The cost related limitations of the first generation solar cells has shifted the focus of the researchers on the development of more cost effective second generation thin film solar cells [9]. The trick behind the reduction in costs of these solar cells lies in the use of less material for their generation. The thin films are only a few micrometers thick which is much less than the crystalline silicon based cells. So use of less material and lower manufacturing costs enables manufacturers to produce and hence sell panels at a comparatively much lower cost.

The second generation includes amorphous silicon (mentioned above) and two more that are made up of non-silicon materials – cadmium telluride (CdTe) and copper indium gallium di selenide (CIGS). These solar cells are fabricated by sputtering, physical vapour deposition, and plasma-enhanced chemical vapour deposition. The highest recorded efficiency is as good as 19.6% [9], which is not very far from the crystalline silicon results. This combination of moderately high efficiency and low manufacturing costs makes the second generation solar cells a good area of interest for the researchers.

1.3.3 Third Generation:-

This generation marked a completely new era in the development of solar cells giving birth to a totally new direction of research and development, i.e. multijunction cells, dye-sensitized cells (DSCs), and organic photovoltaics (OPVs). This approach was also an effort to bring down the costs of solar cells further.

Multijunction solar cells aim at maximising the efficiency and thereby reducing the relative cost or increasing power to cost ratio. These cells contain multiple cells, with different band gaps, stacked over one another so that they can capture maximum region of solar radiation spectrum. A specific combination of the stack can be made to perfectly match the spectrum and result in the efficiency that can even exceed that reported by Shockley and Queisser. The theoretical efficiency limit has reached up to 66% [10]. The laboratories have already witnessed 40% for triple- junction stacked PVs. In 2008, the National Renewable Energy Laboratory (NREL) reported a world record efficiency for a thin triple-junction gallium indium phosphide and gallium indium arsenide cell to be 41.6% [11] (see Figure 1.4).

Organic photovoltaics use polymers for light absorption and even for the PN junction with highest recorded efficiency to be 9.2% [12] .This is not a favourable efficiency however, they can be compensated by their low costs.

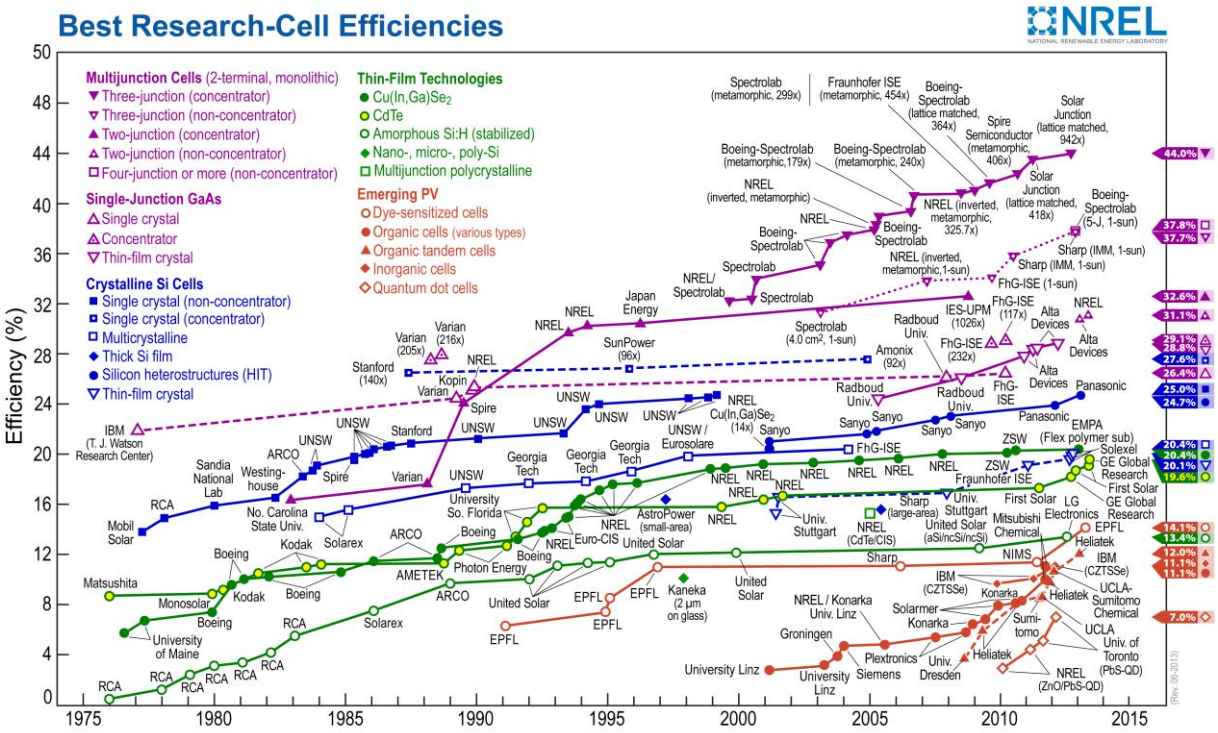

Figure 1.4 The highest recorded efficiencies of a variety of photovoltaic cells [13].

1.4 Organic Photovoltaics:

1.4.1 Importance:-

Organic photovoltaics are solar cells that use organic materials such as polymers (macromolecules) or small molecules. The conjugated polymers combine the advantageous properties of the conventional semiconductors with the comfort of processing and mechanical flexibility of plastics. Hence, this flexi solar cell technology has managed to attract attention in the past few years with the promise of providing environment friendly, flexible, light weighted, inexpensive, efficient solar cells.

The cost reduction of OPVs is mainly due to the solution route, i.e. it employs soluble polymers, and since plastics have high absorption coefficient, very small

quantity of material is needed. Their solubility enables one to use wet-processing techniques like spin coating or roll-to-roll printing (Figure 1.5). Another advantage is that as they are not crystalline in nature, they can be deposited on flexible substrates.

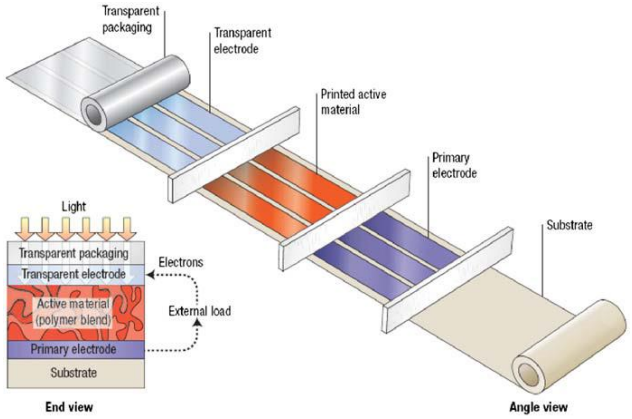

Figure 1.5 Schematic illustration of standard printing processes in polymer solar cells [14].

1.4.2 Different approaches towards OPVs:-

Many different approaches have been successfully employed to produce different types of OPVs.

(a) Dye-sensitized solar cells-

First in this category is dye-sensitized solar cell (DSSC) which consists of an organic dye absorbed at the surface of an inorganic wide gap semiconductor. They gained much attention after Brian O'Regan and Michael Grätzel improved the interfacial area between the organic donor and inorganic acceptor using nanoporous titanium dioxide (TiO_2). This cell is shown in Figure 1.6.

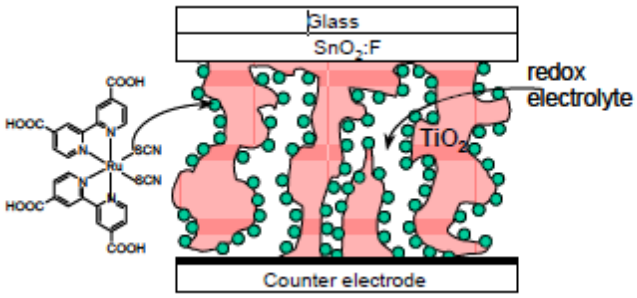

Figure 1.6 *Dye-sensitized solar cell*

(b) Bilayer Planar heterojunction

In this kind of OSC, donor and acceptor bilayer is used as active layer. Power Conversion Effeciency (PCE) of around 1% was achieved by Tang [15-17] by introducing this concept to the OPV cell in 1979.

(c) Bulk heterojunction (BHJ) cells-

The planar junction concept explained earlier has certain limitations- the need of a long carrier lifetime to ensure that the holes and electrons reach their respective electrodes and a small surface area between the donor-acceptor interfaces. This problem has been addressed by introducing a bulk heterojunction. This involves mixing of donor and acceptor materials in the bulk body of the organic solar cell. In 1995 by the groups of Heeger and Friend independently realized the first efficient heterojunction cell in polymer-fullerene and polymer-polymer blends [18,19].

In these cells, the p-type and n-type layers are combined together forming the p-n junction in the active layer. The greatest concern is that the excitons so generated diffuse to the interface to allow charge separation. But due to their low mobility and short lifetime, the diffusion length is just restricted to ~10nm. Thus for efficient charge generation the distance between the interface and the charge generation site must be of the order of the diffusion length of the exciton. This exciton diffusion is visually depicted in Figure 1.7. Thus, the exciton has to reach a nearest donor-acceptor interface within a few nanometers otherwise it will be lost via recombination thus leading to no charge generation (see Figure 1.7). It was found that even a 20nm thick layer of the active materials was not sufficient enough for efficient photon absorption.

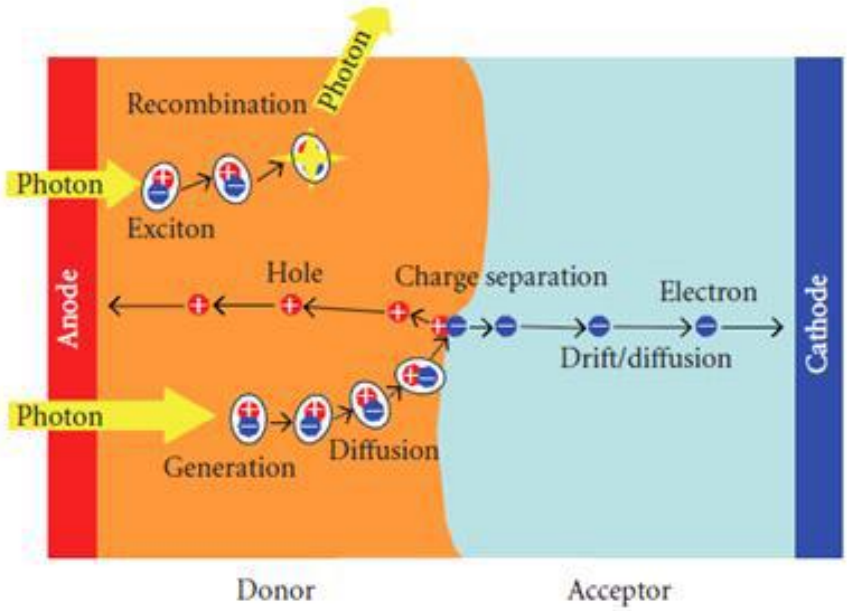

Figure 1.7 Exciton diffusion towards the acceptor-donor interface

So on one hand a thick layer would interrupt the charge separation due to short diffusion lengths of excitons and on the other hand a thin layer would affect the photon absorption. This dilemma was then dealt with a new approach of manufacturing solar cells i.e. by mixing the p and n type materials in the form of a blend and letting the polymers create junctions throughout the bulk of the material, hence ensuring quantitative dissociation of excitons.

The continuous progress in the PCE of BHJ can be observed from Figure 1.4. PCE of bulk heterojunction (BHJ) based polymer solar cells has exceeded 9% [20] in 2012, but it is still much below the value for inorganic solar cells, and in addition, their lifetime is significantly shorter which is major obstacle in their commercialization. However it is predicted that the efficiency of organic solar cells will cross 12% by 2015 or before (see Figure 1.4) and expected to be commercialized very soon.

In a BHJ solar cell a bi-continuous interpenetration network of the polymer and the acceptor is utilized (Figure 1.9) [20]. A major challenge in this approach was to enable a smooth and effective migration of charge carriers towards their respective electrodes. So, these layers should be mixed into a bi-continuous network in which the inclusions or barrier layers are avoided.

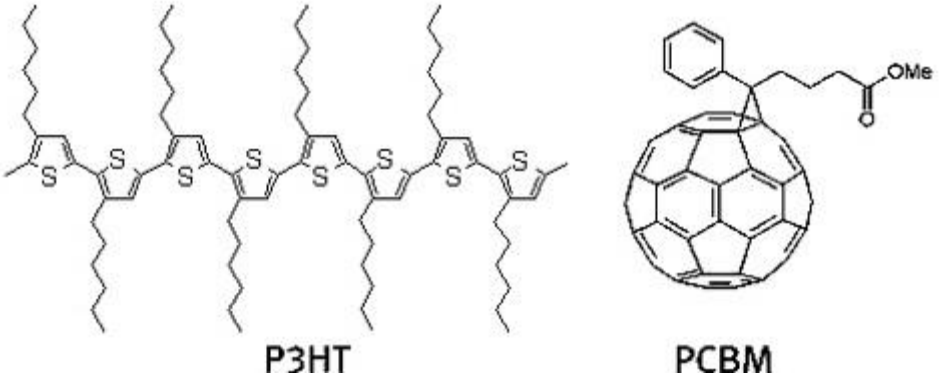

Figure 1.8 The polymer poly (3-hexylthiophene) (P3HT) and the fullerene [6,6]-phenyl-C_{61} butyric acid methyl ester (PCBM)

In this type, the interface or the heterojunctions are all over the surface or the bulk, hence the name bulk heterojunction.

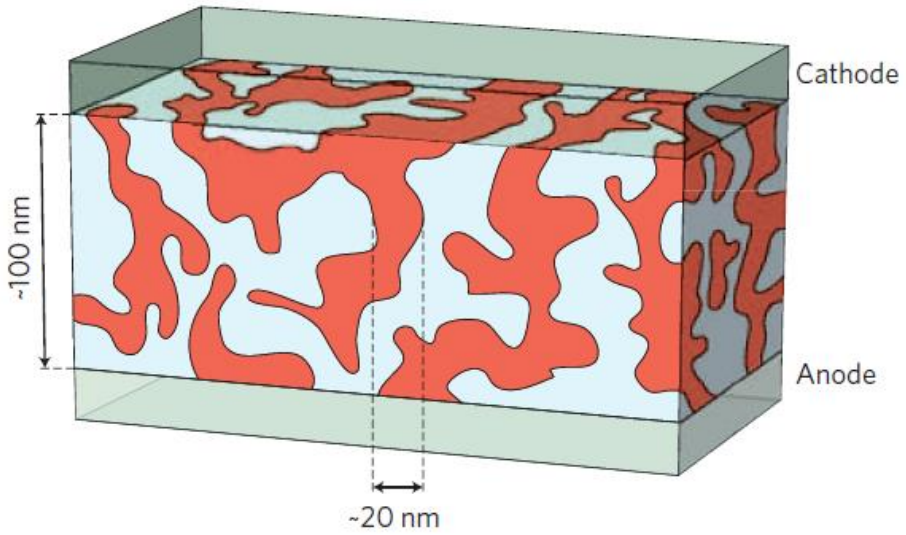

Figure 1.9 Bi-continuous interpenetration network of the polymer and the acceptor [20]

When the photons are incident over the photoactive material, charge transfer occurs due to the mixing of the donor and acceptor material (plane and red area in Figure 1.9). The generated charges are then transported and collected at the respective electrodes. Even though the BHJ concept is powerful as a solution for addressing the issue of exciton dissociation, in 2005 researchers discovered that the morphology (donor-acceptor phase separation) also plays a important role in achieving good charge transport channels for collecting electrons and holes [21,22].

The role of the photoactive layers with the combination mentioned above is quite overwhelming. At their interfaces there occurs a sub-picosecond charge transfer that leads to efficient charge generation. The lifetimes of the chare separated state extends in these blends hence ensuring an effective diffusion of the generated carriers away from the interface towards the electrodes. This cell is explained in more detail in the organic photovoltaic theory part of this thesis. Our work in this thesis is focussed on BHJ based on interface layer modifications using polyelectrolytes.

Chapter 2

Literature Review

2.1 Inorganic Photovoltaic Theory:

In inorganic photovoltaic, a p-n junction is responsible for free charge generation on the arrival of photons from the external light source. A p-n junction is a simple interface between a p type (excess holes) and n type (excess electrons) semiconductor (see Figure 2.1). A p type semiconductor can be formed by diffusing boron (three valance electrons) into silicon. This causes the generation of positive (hole) carriers throughout the lattice. N type semiconductor can be formed by doping phosphorous into the silicon wafer. This doping causes generation of excess electrons in the silicon lattice.

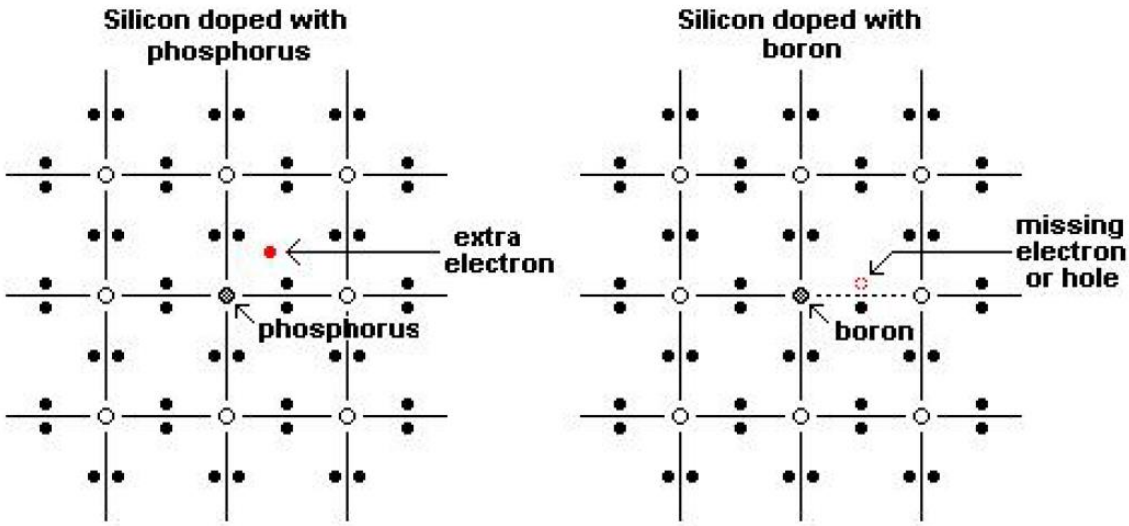

Figure 2.1 From left to right: n and p-type doping of silicon wafer.

When an N-type and P-type material are kept together to form a junction, the electrons from the N-type diffuse into the P-type and the holes from the P-type diffuse into the N-type. Thus, positive ions are left behind in the N-side and negative ions in the P-side. This region is devoid of any free charge carriers (electrons and holes). This region is called the depletion region. This process can be visually depicted as shown in Figure 2.2.

Valence electrons in Si absorb the incoming photons from an external light source. Photons with adequate energy excite the electrons across the forbidden gap into the conduction band. Thus, these electrons being free in nature can be channelled through an external circuit producing current.

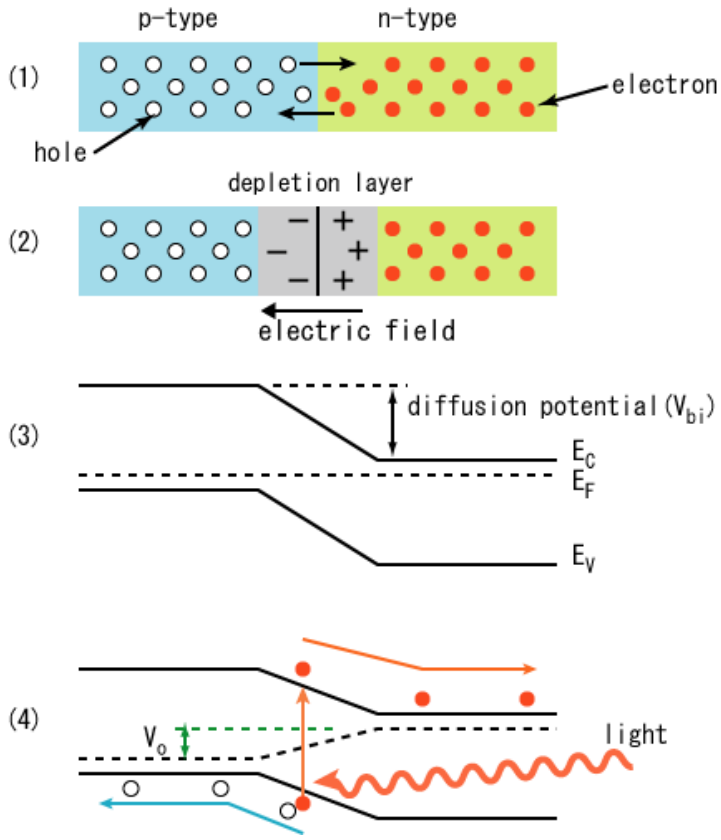

Figure 2.2 The pn-junction of an inorganic solar cell (open circuit); 1) electrons close to the junction, or boundary, diffuse into the p-type region; 2) charge builds up along the interface of the two materials, creating an electric field that opposes the flow of electrons; 3) the conduction and valence bands; 4) a photon excites an electron into the conduction band, and the electron and its positive hole are forced to opposite ends of the cell by the intrinsic electric field

2.2 Organic Photovoltaic Theory:

At first glance it looks as the organic photovoltaic cells work similar to inorganic photovoltaic cells but on closer inspection we notice that there are significant differences between the two photo-conversion mechanisms. Here in organic photovoltaic, absorption of photons leads to exciton generation. An exciton is a bound

state of an electron and hole which are attracted to each other by the electrostatic Coulomb force.

PV cell structures based on organic materials differ from that based on inorganic materials. Inorganic semiconductors generally have a high dielectric constant and a low exciton binding energy (Eg. GaAs, BE= 4meV). Thus, at room temperature thermal energy being k_BT = 0.025eV, the excitons generated due to the absorption of a photon dissociate themselves into positive and negative charge carriers. These charge carriers are easily transported due to the existing p-n junction field and the high mobility of the charge carriers. Contrary to that in inorganic materials, in organic materials the dielectric constant is higher along with the exciton binding energies. The exact magnitudes of binding energies still remain a matter for debate. For polydiacetylene 0.5 eV is required to split the exciton and thus dissociation of excitons does not occur at room temperature. To overcome this exact problem organic solar cells utilize two different materials that differ in the electron accepting and electron donating properties. Charges can then be created by photoinduced electron transfer between the two components in the solar cell.

2.3 Basic Processes in an Organic Solar Cell:

When it comes to the working of an organic solar cell (OSC), four basic processes or events can be outlined:

1. Absorption of light
2. Charge transfer and separation of the opposite charges
3. Charge transport
4. Charge collection

The above four processes (in the order mentioned) are responsible for the working of an OSC. Care should be taken that for an efficient collection of photons, the absorption spectrum of the active material in the organic solar cell should match the solar emission spectrum.

Charges are created during the photo-induced electron transfer. Here, the electron is transferred from an electron donor (D) a p-type semiconductor to an electron acceptor (A) an n-type semiconductor with the aid of photons (hυ):

$$D + A + h\upsilon \rightarrow D^* + A \text{ (or } D + A^*) \rightarrow D^{\bullet+} + A^{\bullet-}$$

After the excitation of the donor (D) or the acceptor (A), charge separated states consisting of the radical cation of the donor ($D^{\bullet+}$) and the radical cation of the acceptor ($A^{\bullet-}$) are created.

Also, another important point is that for efficient charge generation, the charge separated state should be the thermodynamically and kinetically most favourite pathway after photo-excitation. Therefore, the photon energy should be used for generation of the charge separated state and is not lost via some other process such as fluorescence or non-radiative decay. The photovoltage (or open-circuit voltage, V_{OC}) is directly linked to the energy difference between the LUMO level of the acceptor and the HOMO level of the donor, thereby providing the primary driving force for charge separation [20].

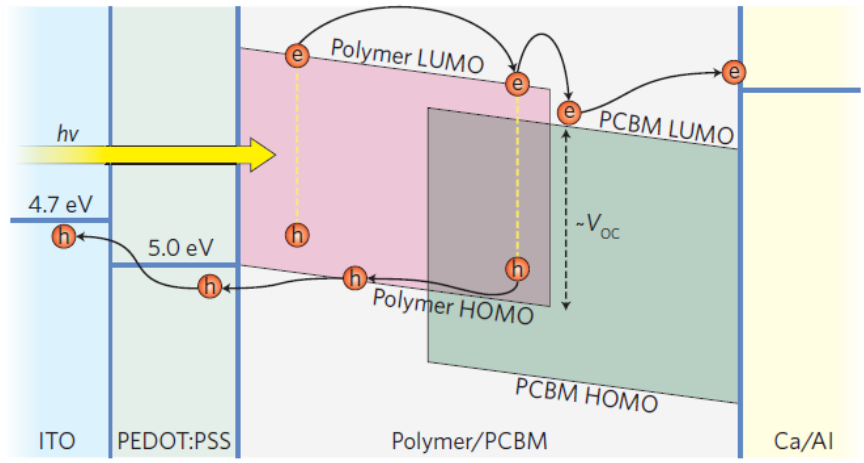

Figure 2.3 Photo-excitation of electrons in donor and the transfer of the electrons into the acceptor; Adapted from [20]

Due to photo-excitation, the electron in the donor moves from the highest occupied molecular orbital (HOMO) to the lowest unoccupied molecular orbital (LUMO) of the donor. This has been shown in Figure 2.3 where ITO is taken as the front electrode with PEDOT:PSS as the buffer layer (or interlayer) and Al as the

metallic back electrode. Consecutively, the electron moves to the LUMO of the acceptor thus creating the charge separated states- $A^{\bullet -}$ and $D^{\bullet +}$. These photo-generated charges are then collected at the opposite electrodes. Similar process can occur when the acceptor is excited instead of the donor material. The donor and the acceptor materials are sandwiched between two dissimilar electrodes, one being a transparent electrode (ITO) and the other a metallic electrode. The structure of organic solar cells is explained in more detail in the next section (Sec. 2.4) of this chapter.

As explained in the previous chapter, among the various approaches to make organic solar cells, bulk heterojunction cells prove to be one amongst the best performing solar cells to due to the many interfaces formed (between the p-type and n-type materials) in the cell. We have focussed our research on bulk heterojunction cells.

2.4 Structure of a BHJ

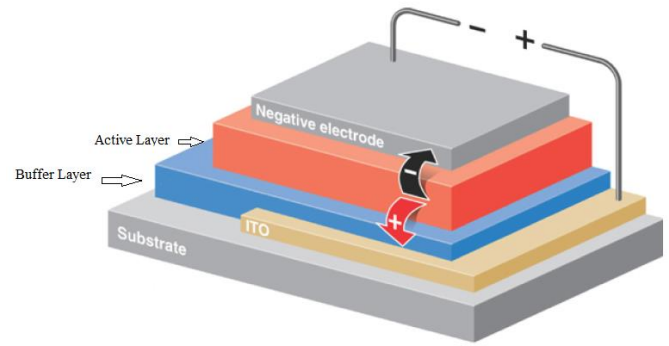

(a)

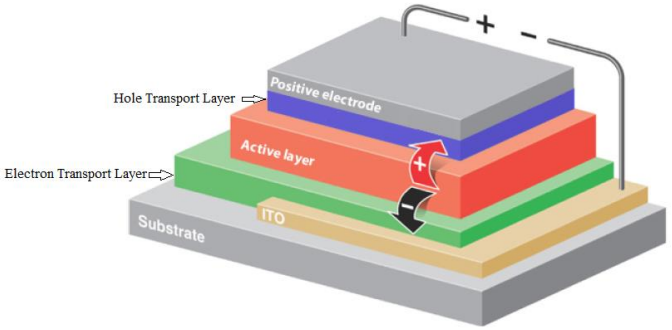

(b)

Figure 2.4 Structure and geometry of bulk heterojunction solar cells **a)** Normal (Conventional) Cell **b)** Inverted cell

2.4.1 Geometry of Organic Solar Cell:

We have two different geometries- normal (or conventional) cell and inverted cell. In a normal cell electrons move towards the metallic electrode which has a lower work function compared to indium tin oxide (ITO) making this electrode as cathode. Whereas, in an inverted cell electrons move towards ITO. Here ITO functions as the cathode. These two geometries are depicted in Figure 2.4.

Both the geometries have their pros and cons of using them. The normal cell features higher efficiencies (recently even inverted cells are known to be highly efficient). The inverted cell being highly stable and can even last for months without much degradation. Inverted devices apart from being more stable are also now as efficient as conventional devices. In inverted devices the electrodes are interchanged i.e. ITO becomes the cathode and the metallic electrode becomes the anode. In these devices, electrons flow towards ITO and holes move towards the metallic back electrode.

2.4.2 Active Layer:

The active layer is where the interfaces between the p-type and n-type materials are made. Here the excitons are generated on photo-excitation. These excitons generated, diffuse into the interface where charge separation occurs. This distance to the interface must be shorter than the exciton diffusion length. In case the exciton length is insufficient, the exciton loses all its energy i.e. recombination occurs even before it reaches the interface. Thus, no charge separation is able to occur in this scenario. Due to low mobility and short lifetime in case of single exciton diffusion, the diffusion length in organic semiconductors is about 8.0 ± 0.3 nm [23].

So, as stated above the active layer is comprised of two materials- p-type and n-type materials. Due to their intrinsic tendency to phase separate on the nano-scale, junctions (or interfaces) throughout the bulk of the layer are created.

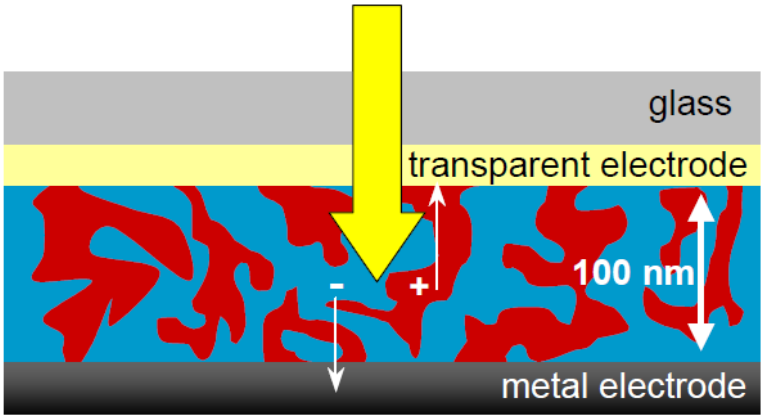

Figure 2.5 Diagram depicting the junctions present in the active layer [24]

To prepare the active layer, the donor and the acceptor materials are mixed in a particular weight ratio. Once mixed in the proper solvent, the prepared solution is allowed to stir for many hours. These materials should be mixed into a bi-continuous, interpenetrating network for the proper formation of junctions and pathways for exciton diffusion. See Figure 2.5. This kind of bulk heterojunction was first explained by Yu et al. in 1995 [25].

2.4.3 Electrodes:

Every organic solar cell consists of two electrodes- the front electrode and the back electrode. In case of normal (or conventional) structure, the front electrode collects holes and the back electrode needs to have a higher work function. In case of inverted structure, the front electrode collects electrons. Here, the back electrode needs to have a lower work function compared to the front electrode.

ITO is used as the transparent front electrode. The front of the cell needs to be transparent in order allow maximum light to reach the active layer. CVD (chemical vapour deposition) graphene is a suitable alternative to ITO. The work functions of ITO and grapheme are 4.8 eV[26] and 4.5 eV[27]. They have mid-range work functions and thus can serve as either anode or cathode. Al has a low work function (4.1 eV[23]) and is generally used as the cathode. Certain thin interlayers such as Ca, CsF, or LiF(~1nm) film thermally evaporated on Al are known to provide better performance [28]. Apart from these layers having a lower work function, they also act as a protective layer between aluminium and the active layer.

2.4.4 Intermediate Layers and device structures:

The contribution of intermediate layers in OPVs is enormous. In the conventional structure of organic solar cells usually PEDOT:PSS or poly(3,4-ethylenedioxythiophene) poly(styrenesulfonate), a conjugated polymer, is used as a hole conducting layer between the active layer and ITO (Figure 2.6) [29].

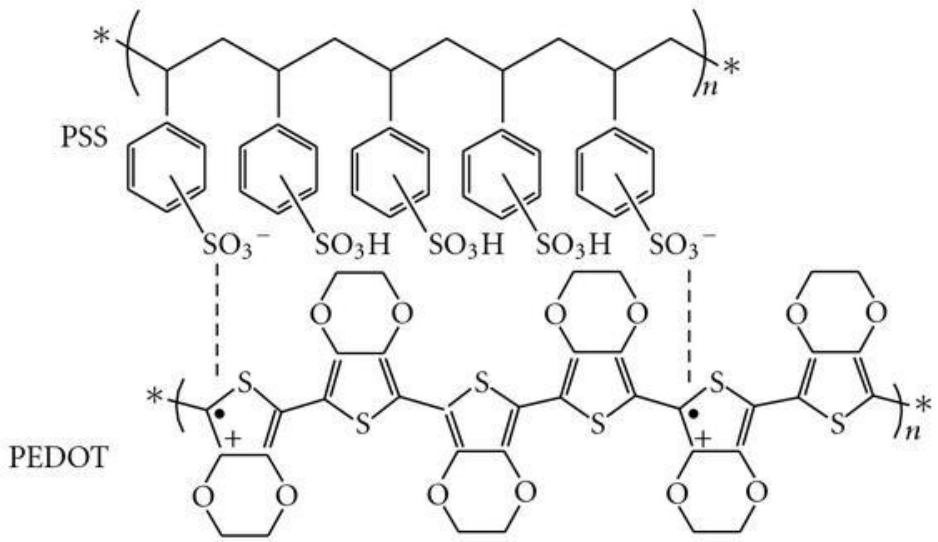

Figure 2.6 The chemical structure of poly(3,4-ethylenedioxythiophene) poly(styrenesulfonate) (PEDOT:PSS) [30]

Electron conducting layers include zinc or titanium dioxide nanoparticles. Based on the structure of the device we determine whether a hole conducting layer is required or an electron conducting layer. Different intermediate layers can be seen for conventional and inverted structures of organic solar cells in Figure 2.4.

Intermediate layers perform many functions. They permit a single type of charge to pass thus, blocking the opposite charges, and hence prevent recombination i.e. an electron transport layer would act as a hole blocking layer and vice-versa.

The intermediate layers may act as steps for electrons or holes as they move from the active layer to the electrodes with unaligned energy levels. Also, these layers on top of the rough ITO, prevent shunts and does not allow any alternative paths for current to pass [31]. The ITO is made rough for maximum photon scattering. It is well known that the electrical properties of intermediate layers are very important for the performance of the devices as they will affect charge transport at the interface. The conductivity of wide bandgap metal oxides (e.g., ZnO and TiO_2) are sensitive to UV light [32-35].

In our investigation, we are using new ZnO-polymer nanocomposites as electron transport (or conducting) layers such as- ZnO-PSS and ZnO-PDADMAC. These layers offer better device performance when used as ETL compared to pure ZnO film.

Table 2.1 Different materials used in conventional and inverted device structures

Cell Structure	**ETL**	**HTL**	**Anode**	**Cathode**
Conventional	Ca,CsF,LiF	PEDOT:PSS	ITO	Al, Ag, Au
Inverted	ZnO, TiO_2	MoO_3	Al, Ag, Au	ITO

2.5 Motivation

Interface layers have various functions in BHJ cells such as:

- They are able to reduce energy barrier between active layer and electrodes and can promote the formation of ohmic contacts for effective charge collection.
- They can form selective contacts for charge carriers.
- They can modify the electrode work function and can change conventional structure to inverted structure.
- They can protect active layer and can modify the field inside.

Generally, PEDOT:PSS is applied on top of ITO to form the ohmic contact for the effective charge collection but acidic nature of PEDOT:PSS creates problems and

researchers have tried various metal oxides such as MoO_3, V_2O_5, WO_3 and NiO. However, solution processed metal oxide has become popular these days due to their low cost deposition.

Recently n-type inorganic metal oxides such as- TiO_X and ZnO have been shown to be good candidates for interface layers in OSCs. Further, the materials with permanent dipole moments can also be used to modify polymer-electrode interfaces. The work function can be increased or decreased by employing polymer layers in view of their electron withdrawing and electron donating properties. By controlling the dipole moment of polymer layers, one can improve efficiency of BHJ using ZnO combined with polyelectrolytes. Polyelectrolytes maybe other successful candidates for the modification of the polymer-electrode interface. Some groups have demonstrated that efficiency of BHJ can be increased by using polyelectrolytes as interface layer for devices based on different polymers [36,37]. In view of above said observations we also motivated to work on the replacement of interface layer by a combination of ZnO and polyelectrolyte based nanocomposite. We have chosen the two combinations of ZnO with polyelectrolytes viz.

- ZnO-PSS
- ZnO-PDADMAC

2.6 Characterization

Characterization of solar cells is carried out by measuring the current against different values of voltage across the cell. An ideal solar cell resembles a diode connected in parallel with a current source. When no light is incident on the cell, the I V characteristics of the cell resemble to that of a diode. Most of the information can be deducted from the IV characteristics under dark as well as light conditions.

On light absorption, current is generated in the device. The power generated is given by,

$$P = I\,V, \tag{1}$$

Where I is the current and V is the voltage, maxim power generated can be calculated from the I V curve.

Power conversion efficiency (PCE) (η) can be calculated using the relation,

$$\eta = \frac{I_{sc} \times V_{oc} \times \mathrm{FF}}{P_{light}} \tag{2}$$

Fill factor (FF) is also an essential parameter in determining the solar cell performance. It is the ratio of maximum measured power to maximum theoretical power. Fill factor (FF) is given by

$$FF = \frac{I_{max} V_{max}}{I_{SC} V_{OC}} \tag{3}$$

Where, I_{SC} is the short circuit current i.e. the current when voltage equals zero and V_{OC} is the open circuit voltage i.e. the voltage when current equals zero.

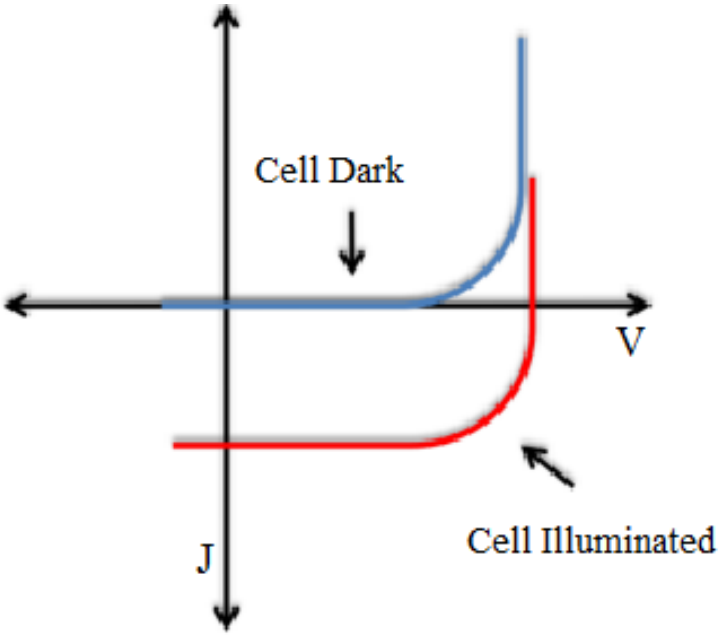

Figure 2.7 J-V curves of an illuminated and dark solar cell; adapted from [38]

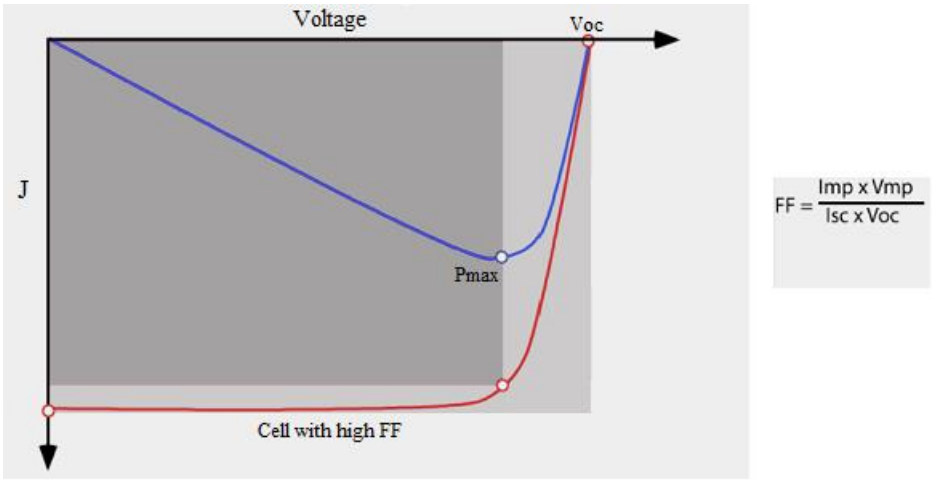

Figure 2.8 Visual illustration of fill factor (FF); adapted from [39].

In order to simplify the internal working of the solar cell, the cell can be modelled into an equivalent circuit consisting of a diode connected in parallel with a current source along with series and shunt resistance. This is shown in Figure 2.9

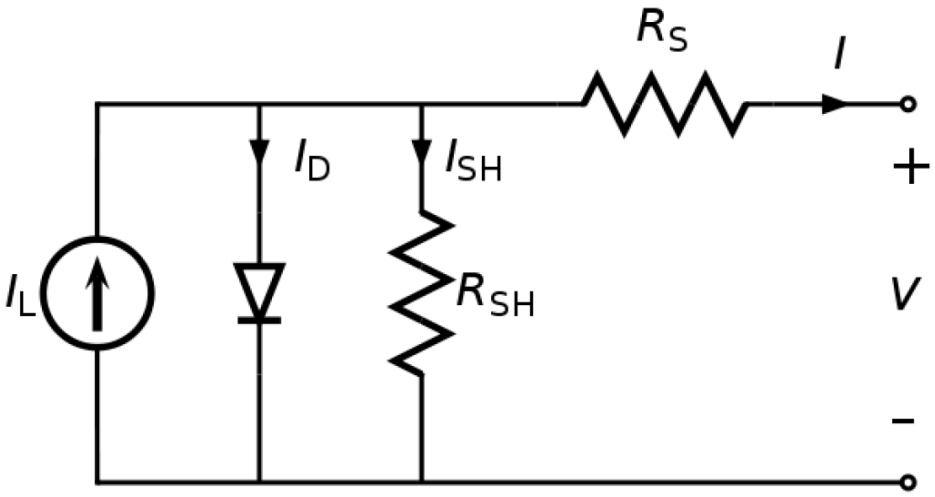

Figure 2.9 An equivalent circuit of a solar cell; adapted from [38].

The equation for current from this model is:

$$I = I_l - I_o(e^{\frac{q(V+IR_S}{nkT}} - 1) - \frac{V + IR_S}{R_{SH}} \quad (4)$$

Where, Io is the diode's saturation current, n is the diode's ideality factor, q is the electron's charge, k is Boltzmann's constant, T is temperature, R_S is the series resistance, and R_{SH} is the shunt resistance.

This characteristic equation can be written in the form of current density (J) as:

$$J = J_L - J_0 \left\{ \exp\left[\frac{q(V + Jr_S)}{nkT} \right] - 1 \right\} - \frac{V + Jr_S}{r_{SH}} \tag{5}$$

R_S (or r_S) and R_{SH}(or r_{SH}) values affect the fill factor of the solar cell as shown in Figure 2.10.

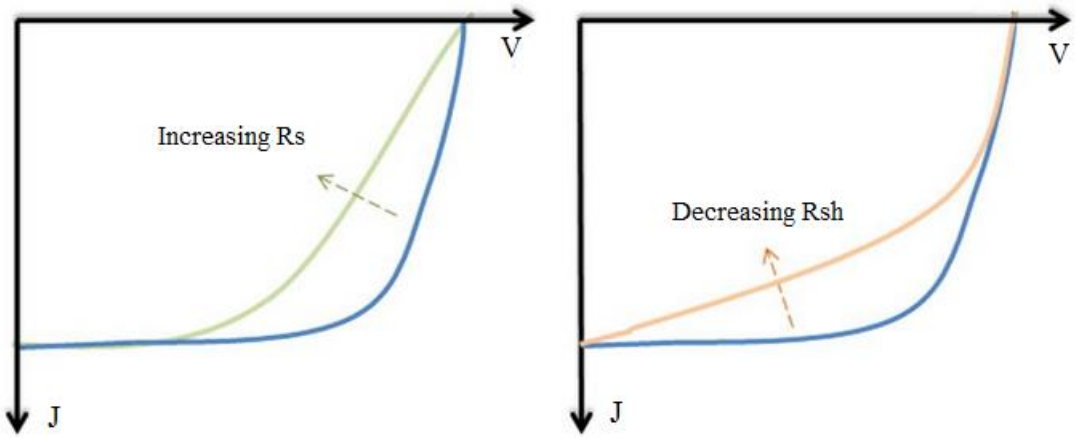

Figure 2.10 Effect of R_{SH} and R_S on solar cell; adapted from [38].

Chapter 3

Materials and Experimental Techniques

3.1 Cell Structure of the investigated device:

Along with the geometry, the different layers used in the devices investigated in this thesis are discussed in this section.

3.1.1 Geometry:-

The organic solar cells investigated in this thesis are based on both conventional as well as inverted structure. The conventional cells have the structure ITO/PEDOT: PSS/P3HT:PCBM/Al, ITO|MoO_3|P3HT:PCBM|Al. The inverted cell has the structure ITO|ZnO|P3HT:PCBM|MoO_3|Al, ITO|ZnO+PDADMAC|P3HT:PCBM|MoO_3|Al, ITO|ZnO+PSS|P3HT:PCBM|MoO_3|Al. In cells based on normal geometry the transparent ITO electrode behaves as the anode (hole collector) and the back Al electrode serves as the cathode (electron collector). In cells based on inverted geometry, ITO serves as the cathode whereas Al serves as the anode.

3.1.2 The Active Layer:-

For our investigation, we have used donor and acceptor combinations mentioned in literature viz; P3HT:PC_{60}BM and PCDTBT:PC_{71}BM whose chemical structures are shown in Figure 3.1. All these chemicals were commercially bought from Sigma-Aldrich, USA. In this thesis, the role of P3HT as the donor polymer has been investigated. P3HT is a widely used semiconducting polymer in polymer solar cells. P3HT is based on thiophene units joined at the 2 and 5 positions in a head-to-tail geometry (Figure 3.1(a)). To be able to dissolve the thiophene a hexyl site group is added in the third position.

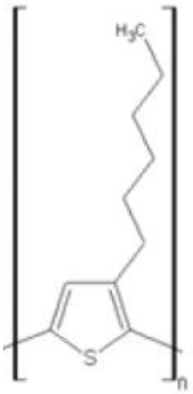

P3HT

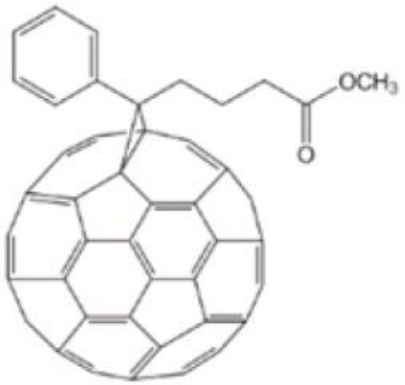

$PC_{60}BM$

(a) **(b)**

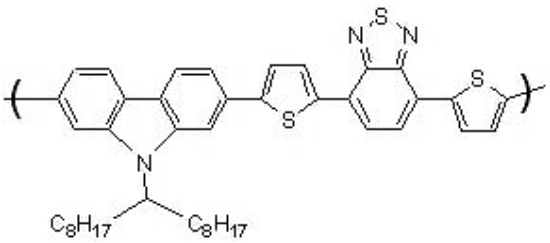

PCDTBT

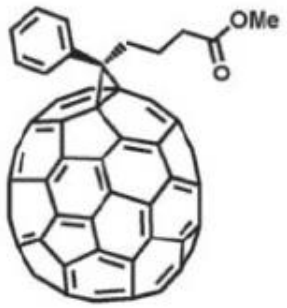

$PC_{71}BM$

(c) **(d)**

Figure 3.1 Chemical structure of (a) donor polymer P3HT (b) acceptor $PC_{60}BM$ (c) donor polymer PCDTBT and (d) acceptor $PC_{71}BM$

P3HT is semi crystalline in solid state. It has a maximum absorption around 500 nm [40]. Due to its electron rich nature and high-energy HOMO level it's a good hole conductor [40]. For a good acceptor, organic materials with high electron affinity are required. Such materials are rare and thus making the choice of acceptors limited [40]. The material investigated in this thesis as acceptor is phenyl [6,6]- C_{61}-butyric acid methyl ester (PCBM) - a soluble C_{60} based compound (Fig 3.1(b)). PCBM forms crystalline domains in the bulk heterojunction with P3HT and it increases the hole mobility of the polymer.

PCDTBT is basically an amorphous polymer. If we compare the two donor polymers, BHJ solar cells with a PCDTBT:PCBM have much better thermal and air stability than those with a P3HT:PCBM BHJ [41] .

3.1.3 Electrode Materials:-

The following are the requirements for a good electrode (cathode and anode):

- A large difference in the work function of the electrode materials can give rise to a large V_{OC}.
- The front electrode needs to be transparent in order to allow maximum light to enter the active layer and cause photo generation of charge carriers.
- The back electrode is usually a metallic and opaque material.

In view of these requirements we chose Indium Tin Oxide (ITO) as the front electrode and Al as the metallic back electrode. Umicore, a company that specializes in thin film products specifies that the front electrode which is ITO electrode has typical composition ratios of In_2O_3/SnO_2-95/5, 90/10 and 83/17 wt% with a band gap of 3.7eV. Here, sheet of resistivity- 4 to 8 $\Omega \cdot sq^{-1}$ is used. The current densities vary from 5-10 $mA \cdot cm^{-2}$. Further, the work function of ITO depends upon the inter layer above the ITO such as- PEDOT:PSS and ZnO.

3.1.4 Buffer Layers (or interlayers):-

In view of improving the charge transport at the interface between the electrode and the active layer we use buffer layers. This layer facilitates the following functions:

- It protects the organic layer from diffusion of the electrode material into it.
- It prevents the penetration of oxygen and water molecules.

We have chosen PEDOT:PSS, MoO_3, ZnO and ZnO with polymers namely - PSS and PDADMAC as the buffer layers for our devices.

Poly-(ethylenedioxythiophene):polystyrensulphonic acid (PEDOT:PSS), which is a hole transporting layer is inserted between the ITO and the active layer. The chemical structure of PEDOT:PSS is shown in Figure 3.2. Along with making the surface uniform, it also enhances the adhesion of the organic active layer onto the ITO (anode).

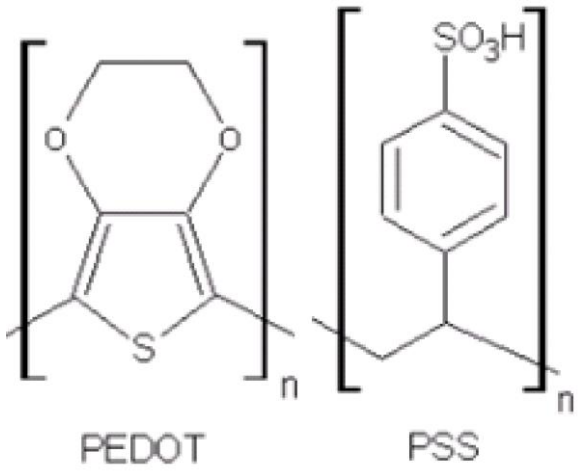

Figure 3.2 Chemical structure of the donor polymer PEDOT and the acceptor PSS

The PEDOT:PSS film is semi-transparent with light blue colour. In terms of conductivity, this layer is able to attain values comparable to that of metals [42]. Along with certain advantages, there are a couple of disadvantages too- due to the hygroscopic nature of PEDOT:PSS, water is introduced in the cell which later causes degradation in organic solar cell. PEDOT:PSS is used as a hole transport layer (HTL). Its work function is around 5.1 eV which is 0.4 eV higher than that of ITO (4.7 eV). This thus leads to a reduction in the injection barrier between the ITO and the active layer. Before coating PEDOT:PSS, UV-ozone treatment of the ITO substrates is usually carried out. This is done to make the ITO surface hydrophilic and to reduce the contact angle with water (discussed in section 4.5). PEDOT:PSS is widely used due to its several advantages such as- high work function (~5.2eV), good conductivity and highly stable oxidized state [43-48].

3.1.5 Polymers

Poly(4-styrenesulfonic acid) or PSS

Poly(4-styrenesulfonic acid) (PSS) polymer has many medical applications. The chemical structure of PSS is shown in Figure 3.3. They are used to remove high levels of potassium from blood. PSS is soluble in water.

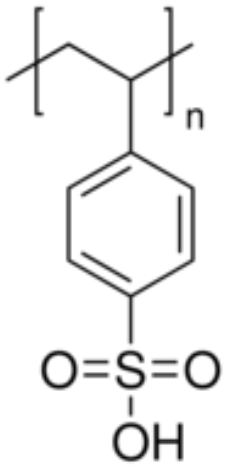

Figure 3.3 Structure of Poly(4-styrenesulfonic acid) (or PSS)

Poly(diallyldimythylammonium chloride) or PDADMAC

Poly(diallyldimythylammonium chloride) (PDADMAC) is a polymer of diallyldimethylammonium chloride (DADMAC). The chemical structure is shown in Figure 3.4. It is a high charge density cationic polymer and thus making it suitable for flocculation. It too is soluble in water.

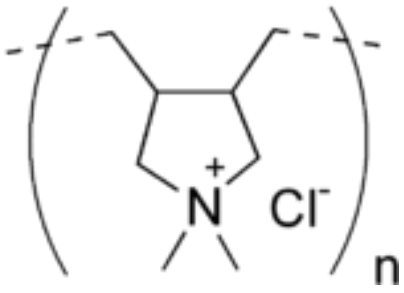

Figure 3.4 Structure of Poly(diallyldimythylammonium chloride) (PDADMAC)

3.2 Experimental Techniques Used:

3.2.1 Standard Glove Box

Due to hygroscopic nature of materials used for organic solar cell fabrication we need to use a glove box with high purity inert atmosphere (such as nitrogen or argon). Figure 3.5 shows the MBrawn standard glove box used in NPL, New Delhi. The gloves are placed in such a way that the user can place both arms inside and carry out the necessary task inside the glove box. Glove boxes are also used in cases where hazardous materials need to be dealt with. The samples need to be loaded into the ante chamber first. The working inside the glove box is briefly explained:

Loading materials into the antechamber

- Before loading the materials the antechamber needs to be purged.
- Open the gate of the antechamber and load the materials.
- Once loading is complete, the antechamber needs to be evacuated and purged at least thrice so that all of the oxygen and other non-inert gases are removed from the antechamber.

Transferring the materials from the antechamber into the glove box

- Insert both arms into the glove box and use the left side of the foot pedal to decrease the pressure inside the box.
- Once the antechamber has been purged at least thrice, open the gates of the chamber and make the necessary transfers.
- It is important to check whether any debris is left behind as this could prevent the gates of the antechamber from shutting properly.
- Now close the gates of the antechamber and evacuate it when working inside the box.

Figure 3.5 Picture of Glove Box used in NPL, New Delhi

3.2.2 Spin Coating Technique

The technique of spin coating is one of the most widely used techniques used for coating in organic solar cells. The ease of reproducing homogenous films using this technique is the prime factor. In this technique, the angular velocity of the substrate causes the excess of the solution over the substrate to be ejected. Centripetal acceleration will cause most of the excess fluid to spread up to the edge of the substrate. In the end a thin homogenous layer is obtained over the substrate. Excess of the solution (or ink) is dropped using a dropper onto the centre of the substrate (Figure 3.6 (a)). Then the substrate is made to rotate at the desired rotation speed i.e. rpm (rotations per minute) for a particular time interval. It is possible to reproduce the film thickness, morphology and surface topography if the rotation speed (rpm) and time interval are kept constant.

The key stages in spin coating are - deposition, spin-up, spin-off and evaporation [49]. This is depicted in Figure 3.6(b).

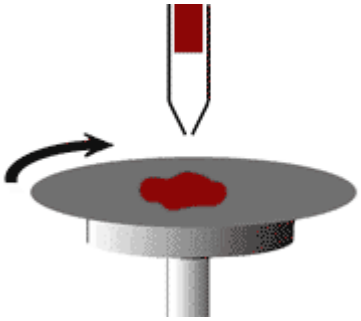

(a)

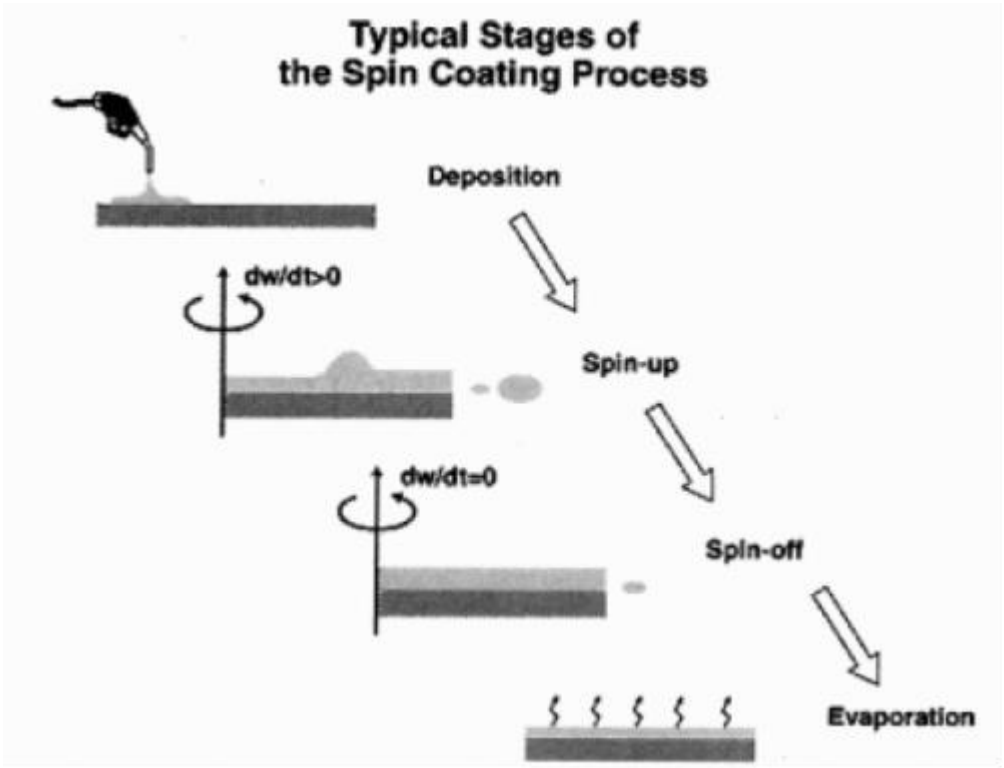

(b)

Figure 3.6 (a) Position of solution deposition **(b)** Stages of spin coating process [49]

The spin coating technique is simple enough for laboratory use but is not efficient enough for industrial use. When it comes to commercialization of organic photovoltaic technology where mass scale production is required, it becomes uncompetitive.

3.2.3 Vacuum Technology

In thermal evaporation (discussed in the next section), vacuum technology plays an essential part. Here the different pump technology used will be discussed, namely-rotary pump and turbo pump.

a) Rotary Vane Pump:

The rotary pump is an oil sealed rotary displacement pump. See Figure 3.7. It essentially consists of- a housing (1), an eccentrically installed rotor (2), vanes (3) installed using a spring for radial movement of the rotor, an inlet and outlet (4).

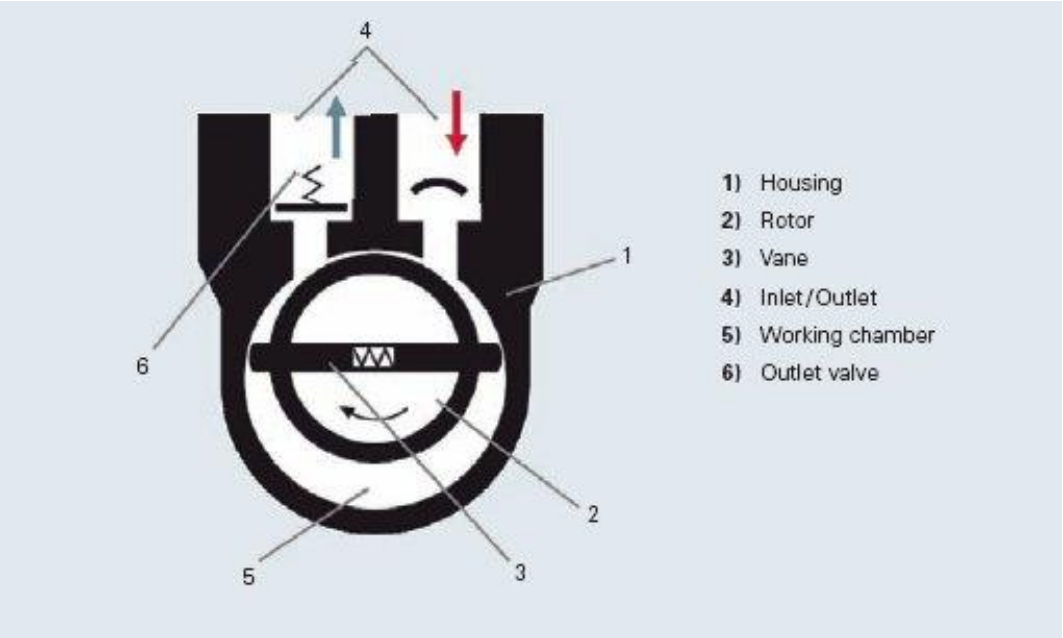

Figure 3.7 A rotary vane pump [50]

The vanes along with the rotor together divide the working chamber into two different spaces with variable volumes. The centres of the rotor and housing are offset thus causing eccentricity. The movement of the rotor leads to two separate variable sized volumes within the working chamber. This in fact gives rise to the pumping action in the motor. The inlet is attached to the space with increasing volume and the outlet is attached to the space with decreasing volume. As the volume of the space increases, a low pressure is generated within the space causing air to flow in from the inlet. Whereas, when the volume in the second space within the working chamber decreases,

a high pressure is generated within thus causing the air to be expelled from the outlet connected.

b) Turbomolecular Pump:

Turbomolecular pumps come under the category of kinetic pumps. They are used in ultra-high vacuum (UHV) systems. The mechanism used in this pump is based on the fact that molecules can be given momentum in a particular direction by repeated collision with a solid surface. A rapidly spinning rotor (similar to a turbine rotor) repeatedly hits the gas molecules from the inlet and towards the exhaust. Figure 3.8 shows the lateral view of the inside of a turbomolecular pump. This pump consists of stack of rotor disks. In between rotor disks are stators. As the name suggest stators are stationary disks that contain similar blades as the rotors but oriented in the opposite direction.

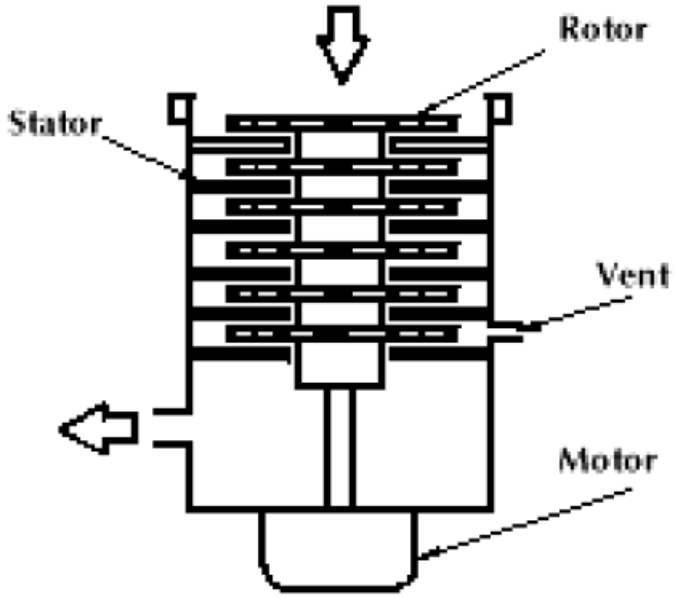

Figure 3.8 Lateral view of turbomolecular pump [51]

3.2.4 Thermal Evaporation Technique:

This technique of deposition incorporates ultra-high vacuum. The material to be deposited is kept on a boat. Here, electric resistance is used to heat the boat to extremely high temperatures. This causes the material kept on the boat to slowly melt and then

evaporate onto the substrates kept above for deposition. The presence of ultra-high vacuum assures the formation of impurity free film on the substrate as impurities of the residual gas present in the working chamber is absent. Also in vacuum the vapour reaches the substrate without any collisions or scattering with other gas phase atoms in the chamber (Figure 3.9).

Thermal evaporation is one of the simplest processes of depositing material onto a substrate. One major drawback is the wastage of the material during deposition.

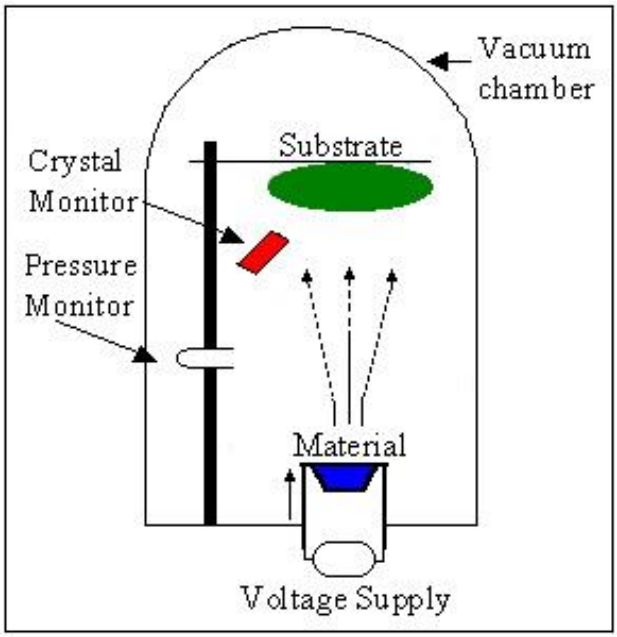

Figure 3.9 Thermal evaporation process

The specifications of the system are mentioned below.

Specifications:-

- Chamber pressure ~ 1 x 10^{-5} to 5 x 10^{-5} mbar.
- Typical filament current varies from 10 to 200 Amps.
- Tungsten or Molybdenum boats used to heat the evaporants.
- Maximum deposition thickness ~ 600 nm.

Chapter 4

BHJ Solar Cell Fabrication

4.1 Etching of the ITO glass sheet:

ITO glass sheets were first cut into 2 X 2 inch substrates using a diamond cutter. These substrates were then subsequently etched using a laser scriber. Two vertical stripes each of 0.6 cm were left out and the remaining ITO was etched. These stripes later helped in the formation of a pixel. In the pattern used, four such pixels were present once device fabrication was complete. Each pixel would function as a different and independent solar cell. Now these patterned ITO substrates need to be thoroughly cleaned before device fabrication.

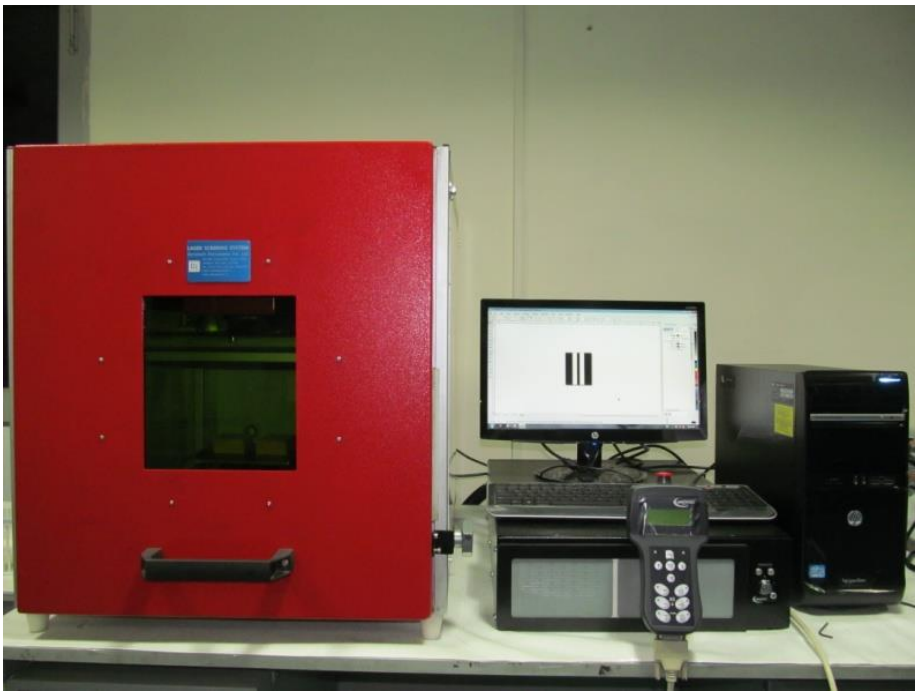

Figure 4.1 Picture of Laser Scribing Unit used in NPL, Delhi

4.2 Preparation of Active Material:

In this thesis two active material (donor polymer: acceptor fullerene combination) have been investigated- P3HT:$PC_{60}BM$ and PCDTBT:$PC_{71}BM$. As

previously discussed in section 3.1.2, both P3HT and PCDTBT are donor polymers whereas both varieties of the fullerene compound ($PC_{60}BM$ and $PC_{71}BM$) behave as acceptors. The weight ratios used for the preparation are:

For P3HT:$PC_{60}BM$- 3:2 wt. ratio

For PCDTBT:$PC_{71}BM$- 1:4 wt. ratio

The solvent used in both the cases is chlorobenzene (each 1 ml).

Both these active layer combinations are stirred using a magnetic stirrer. The P3HT:$PC_{60}BM$ combination was stirred 24 hours of stirring before use whereas the PCDTBT:$PC_{71}BM$ requires minimum 48 hours of stirring before it can be used for coating.

4.3 Preparation of Buffer Layer Solutions:

The buffer layers solutions were synthesized using solution route. The following buffer layers were used for the present investigation

For conventional device-:

- PEDOT:PSS
- MoO_3 film

For inverted device-

- ZnO film
- ZnO - PSS nanocomposite film
- ZnO – PDADMAC nanocomposite film

ZnO Solution

0.235 g of zinc acetate dihydrate was added in 5 ml propanol and allowed to stir for 5 min. A white cloudy solution is obtained here. Now after 5 minutes, few drops of diethanolamine (DEA) are added to this solution. DEA acts as a stabilizer. Slowly we will observe that the cloudiness disappears and a colourless and transparent solution is obtained. Now, this solution is stirred at 60°C for 2 hours. The solution is then kept untouched and undisturbed for 24 hours. After coating this solution on ITO, the substrate is heated at 200°C for 30 minutes.

ZnO-PSS nanocomposite solution

To make PSS solution we added 0.5 ml PSS in 0.5 ml of water. This solution was stirred for 30 minutes. Now to prepare the nanocomposite solution, this 1 ml PSS solution was added in 2 ml of ZnO solution. Also after a 5 minute interval, 2 to 3 drops of DEA were added in this solution and the resultant mixture was then stirred for 30 minutes.

ZnO-PDADMAC nanocomposite solution

To make PDADMAC solution we added 0.5 ml PDADMAC in 0.5 ml of water. This solution was stirred for 30 minutes. Now to prepare the nanocomposite solution, this 1 ml PDADMAC solution was added in 2 ml of ZnO solution. Also after a 5 minute interval, 2 to 3 drops of DEA were added in this solution and the resultant mixture was then stirred for 30 minutes.

All the previously mentioned chemicals were commercially purchased from Sigma Aldrich, USA.

4.4 Cleaning of the ITO glass slide:

First the glass slides were wiped using a tissue dipped in acetone. Here all the dust and other particles are removed from the glass slides (or substrates). Following this, the slides are ultra-sonicated in a beaker filled with soap water. Here further other micro-sized impurities are removed.

Ultrasonic cleaning is the process in which sound is used to produce bubbles by agitation of a liquid (mostly water). This agitation produces high forces on impurities and helps in loosening contaminants tightly adhered to the glass surface [52]. This is allowed to continue for another 20 minutes.

Figure 4.2 Ultrasonic cleaning of substrates (in beaker)

Once the ultrasonic cleaning process is complete, the slides are further rubbed with soap using cotton. This process of rubbing with soap is carried out until a proper thin layer of water stays on the glass surface. This step is particularly done to remove any oil contaminants from the glass surface (as shown in Figure 4.3).

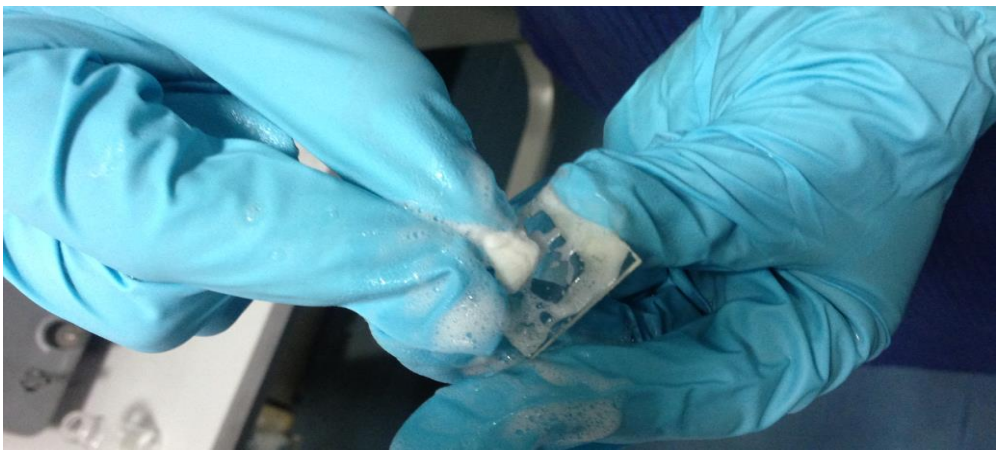

Figure 4.3 Soap Cleaning of ITO substrate

After completion of the above, a three step boiling process is carried out. In the first step the glass substrates are boiled in acetone for 15 to 20 minutes. Boiling is carried out with the help of a substrate holder. Each holder can hold upto 8 ITO substrates (Figure 4.4). Acetone removes all the tiny water droplets that were stuck to the substrate. In the next step these substrates are boiled in trichloroethene (TCE) for another 20 minutes. While making the transfer, the fumes expelled during boiling, aid in substrate drying. TCE removes acetone completely from the glass surface. Also in this

step if any impurities are still left, they can be removed physically using cotton wrapped around a clean tweezer. In the last and final step, the glass substrates are boiled in iso-propanol (ISP) for 15 minutes. Boiling propanol removes the remaining TCE from the substrates.

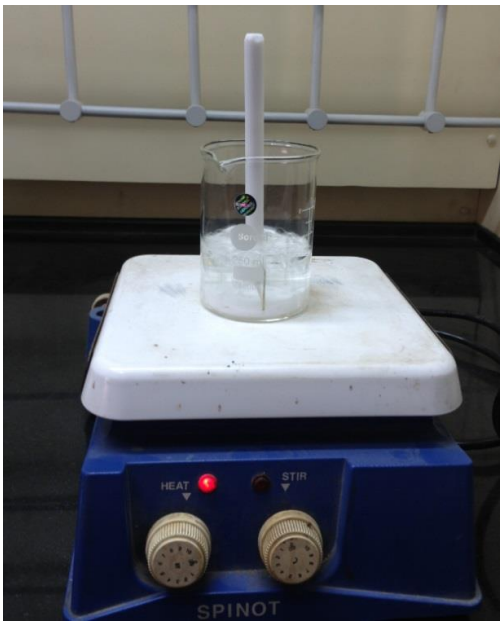

Figure 4.4 Boiling of the ITO substrates

Once the above three steps are completed, the dried glass substrates are kept in a clean petri dish and are kept for drying in the oven at 150°C for 30 minutes.

4.5 UV-Ozone Treatment:

This treatement is undergone in the standard glove box used in Nationl Physical Laboratory (NPL), New delhi. Here we expose the ITO substrates to ozone. ITO is widely used as an electrode material in organic photovoltaics (OPVs). The morphology of the ITO surface and the oxygen defects are known to be important factors in determining the charge injection at the interface [53]. Treatments such as chemical treatment (aquaregia, RCA), and plasma treatment, and UV-ozone treatment have been developed to improve the charge injection from the ITO into the organic layer [54-56]. These treatments can increase the ITO work function, which may be due to surface carbon removal, creation of surface dipoles, a change in the ratio of surface constituents (Sn, In, O). This increase in ITO work function can cause an increase in the hole-injection efficiency from the ITO to the hole-transporting layer [49]. UV-ozone treatment also causes the ITO surface of the substrate to be hydrophilic (i.e. the contact

angle for water decreases) and thus assisting in the uniform and homogenous layer formation over the ITO.

Once the ITO glass substrates are kept face up, the working chamber is closed. Now oxygen gas is purged inside the chamber. This purging takes place for 60 seconds after which UV light is radiated inside the chamber. This converts the existing oxygen gas into ozone gas. The duration for this UV radiation is 600 seconds. Next finally nitrogen gas is passed in the chamber. This is done as once the process completes, the inert gas atmosphere is maintained inside the glove box.

4.6 Buffer Layer Coating:

4.6.1 For conventional cells

Once the UV-ozone treatment of the ITO substrates is completed, the buffer layer coating can begin. The buffer layer used here is a hole transport layer (HTL) as the holes in a conventional structured cell move towards the ITO electrode (anode). The coating technique used here is spin coating. Two HTLs have been investigated, namely- MoO_3 and PEDOT:PSS. However, before spin coating the PEDOT:PSS, it needs to be filtered. PTFE hydrophilic filter was used used for filteration. This filter is attached to a syringe. This system is then used to filter and then drop the PEDOT:PSS solution onto the substrate for spin coating. The equipment used for spin coating is shown in Figure 4.5. Employing PEDOT: PSS has its pros and cons (as discussed in section 3.1.4).

4.6.2 For inverted cells

In case of inverted structure, ZnO films have been coated for investigation. Further, ZnO-PSS and ZnO – PDADMAC nanocomposite films has also been investigated in this thesis. ZnO lowers the work function of the electrode (ITO) and thus the electrons instead of moving towards the metallic electrode, moves towards ITO thus, making ITO the cathode.

Figure 4.5 Picture of Spin Coating System in NPL, New Delhi

4.7 Annealing of Buffer Layer

4.7.1 PEDOT:PSS (For conventional cells)

Once PEDOT:PSS is coated over the ITO substrate, this buffer layer now has to be annealed at 120°C for 10 minutes. This is done so at to dry the PEDOT:PSS layer as it is water soluble. Thermal annealing of PEDOT:PSS is known to increase the short circuit current density and change the work function of the layer [57].

4.7.2 ZnO films (For inverted cells)

ZnO film is based on water and thus needs to be heated at 200°C for up to 30 minutes. This causes all the excess water to boil and evaporate, leaving just the film. Care was taken while cooling the substrate. Cooling was done slowly as abrupt cooling can disturb the surface morphology.

4.8 Active Layer Coating

In this work, P3HT:$PC_{60}BM$ is the active layer used for conventional devices. This active material is a well-known material and has been dynamically used in organic photovoltaics.

While selecting active materials for use, two important parameters are- the absorption of the active material in sunlight as well as the surface morphology after the

coating process is complete. The above two parameters have been studied in detail in the coming chapters. Again the coating method used is spin coating technique similar to PEDOT:PSS. I have selected P3HT:$PC_{60}BM$ for conventional devices and PCDTBT:$PC_{71}BM$ for inverted ones. Reason towards this approach has been discussed in the upcoming sections.

4.9 Active Layer Annealing

Annealing of the active layer is the key to obtaining optimum values of current and fill factor. Annealing of the active layer (both P3HT:$PC_{60}BM$ and PCDTBT:$PC_{71}BM$) was carried out in inert glove box environment (nitrogen environment) at 120°C for 10 minutes. This process should not be carried out in air as oxygen diffuses into the active layer and degrades the material. The changes in surface morphology due to thermal annealing have been noted in the results section. Once annealing is complete next is the thermal evaporation step.

4.10 Thermal Evaporation

In both conventional as well as inverted cells, aluminium is deposited by thermal evaporation. The only additional step required in case of inverted cells is the deposition of MoO_3 just before aluminium. As described in section 3.2.4, this process involves the current heating of a filament (or boat) in a vacuum chamber. Ultra high vacuum (UHV) is needed for this process.

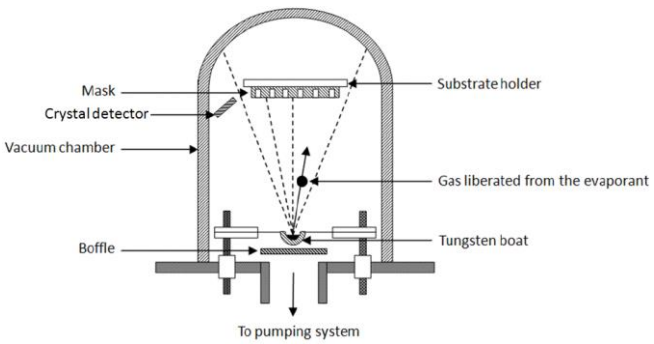

(a) (**b**)

Figure 4.6 (a) Thermal Evaporation Unit and, **(b)** Working of thermal evaporation system at NPL, New Delhi

Pressure up to 9 x 10^{-6} mbar was attained in the chamber. The process specifications used are:

- MoO_3 deposition: (For inverted cells)
    - Power- 30 W
    - Deposition Rate- 0.5 A°/sec
    - Thickness-7.5-8 nm
- Aluminium deposition: (For both-inverted as well as conventional devices)
    - Power-35 W
    - Deposition Rate- 5 A°/sec
    - Thickness-125 nm

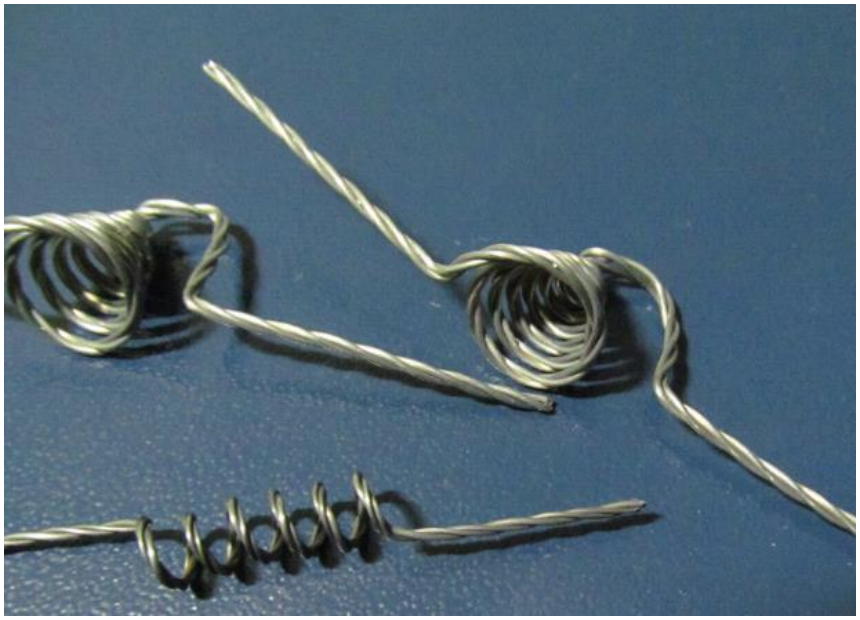

Figure 4.7 Filaments used in thermal deposition process

Once deposition is complete, air is slowly passed into the chamber. The rate is maintained low so as to avoid any major dust particles from entering the chamber and settling on the substrate.

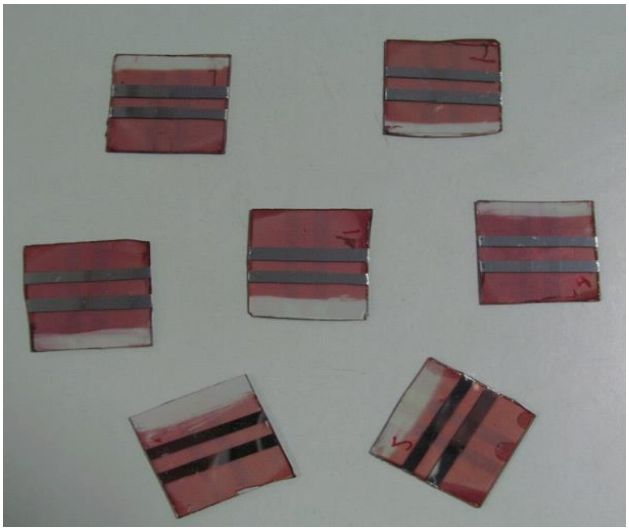

Figure 4.8 Organic Solar Cells Fabricated

4.11 J-V Characterization of the Device

Once the above steps are complete and the device is fabricated, J-V characterization of the device is carried out. Here, the cell is illuminated under simulated AM1.5G Illumination at 100 mW/cm^2 (Figure 4.9) using a light source having tungsten halogen lamp from Osram, Germany. The current density characteristics of the device were recorded using Keithley 2420 SourceMeter interfaced with a computer. The measurements were done both in illuminated and dark conditions.

Depending on the structure of the device, the positive and negative terminals of the Keithley unit are attached with the anode and cathode terminals of the device respectively. Using the current and voltage characteristics fill factor (FF), open circuit voltage (V_{OC}), and power conversion efficiency (η) were measured.

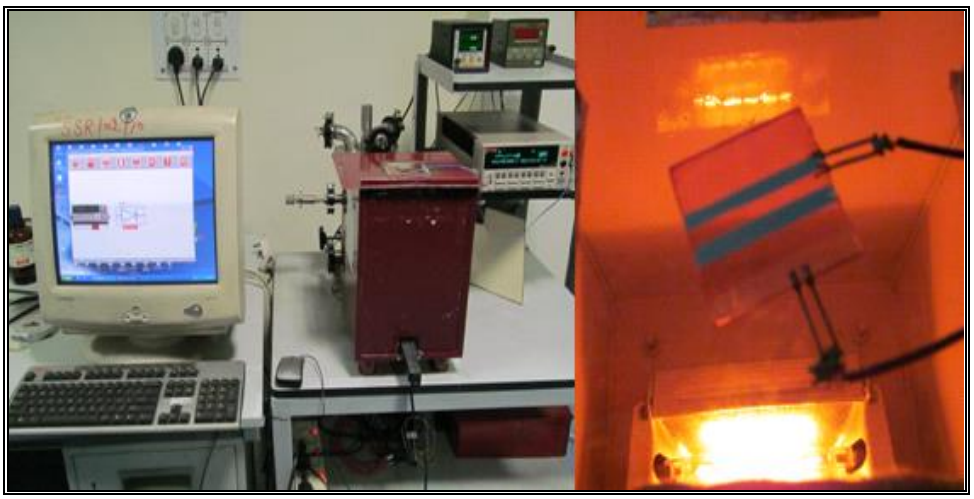

Figure 4.9 Set-up for J-V characterization of the device.

This entire fabrication process is depicted in Figure 4.10.

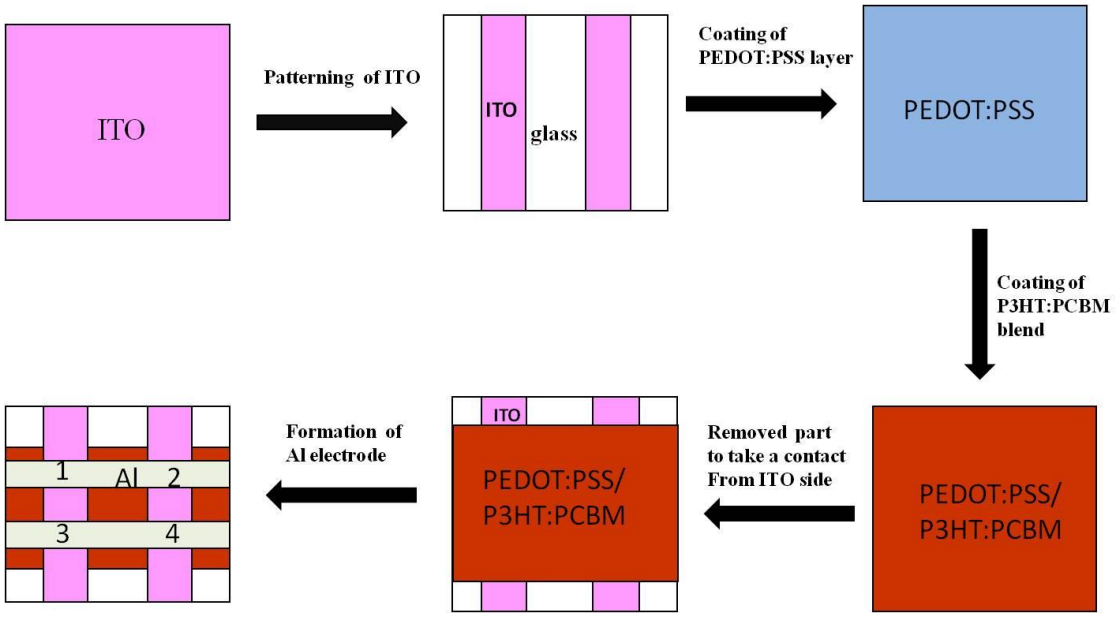

Figure 4.10 Schematic diagram of complete process for fabrication of a typical BHJ solar cell using PEDOT:PSS as the anode buffer layer and P3HT:$PC_{60}BM$ as the active layer.

Chapter 5

Results and Discussion

5.1 Study of Conventional Devices:

It is a well-known fact that conventional devices show inferior stability as compared to inverted devices. Nonetheless, it is important to study both geometries as research in the field of organic photo-voltaic is relatively new. We have started to fabricate device using PEDOT:PSS as the hole transport layer (HTL) and the device structure used is:

ITO|Buffer Layer|P3HT:$PC_{60}BM$|Al

5.1.2 Conventional organic solar cell devices based on PEDOT:PSS as the hole transport layer

We coated PEDOT:PSS on the cleaned ITO substrate at different rotation speeds of spin coater. The device data is presented in Table 5.1. J-V measurements have been carried out at different rotation speeds and the result is represented in Figure 5.1.

We observed that the change of rotation speed of spin coater does not make any difference in the overall device performance. The device parameters (Table 5.1) remain near constant irrespective of the change of rotation speed

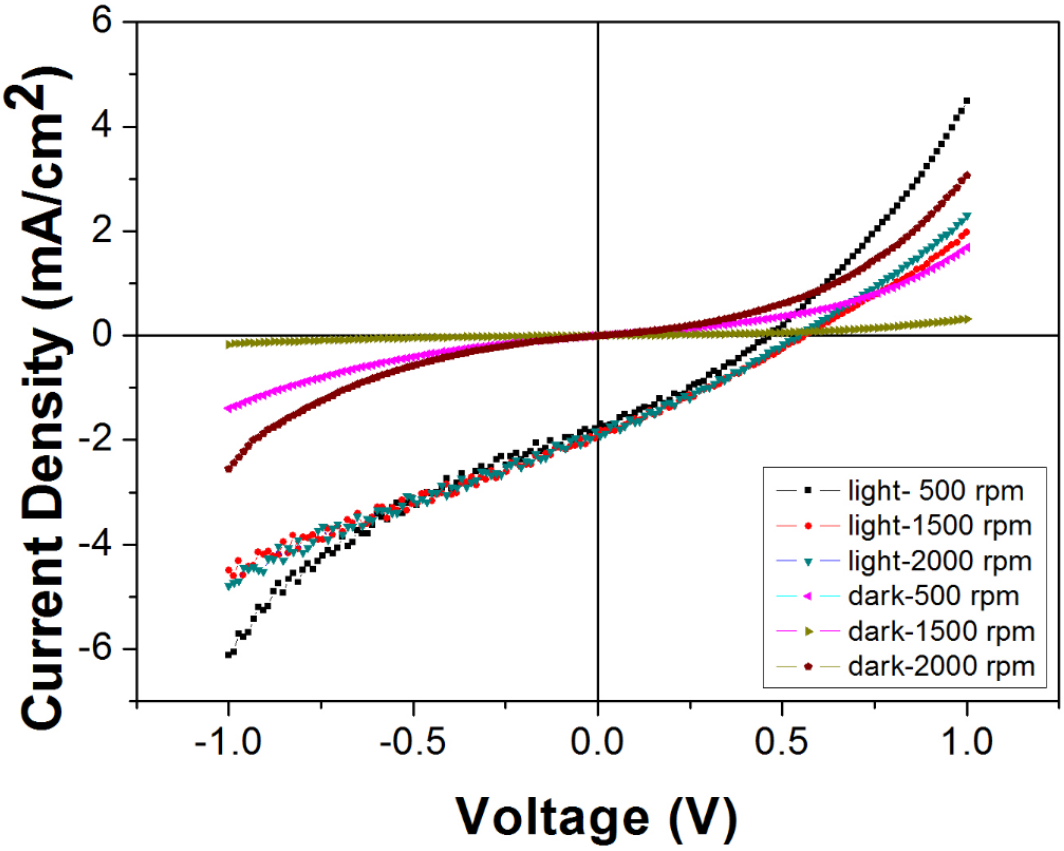

Figure 5.1 J-V plot at different rotation speeds (rpm) of PEDOT:PSS in solar cell with device structure ITO|PEDOT:PSS|P3HT:$PC_{60}BM$|Al

Table 5.1 Device Parameters of ITO|PEDOT:PSS|P3HT:$PC_{60}BM$|Al

Rotation Speed (rpm)	**Fill Factor (FF) (%)**	**V_{OC} (V)**	**J_{SC} (mA/cm^2)**	**PCE (%)**
500	33.6	0.503	1.76	0.297
1500	28	0.557	1.97	0.308
2000	30	0.544	1.83	0.120

It is obvious from Figure 5.1 that the device suffers serious problem of leakage current. The series resistance of the device is also high hence; we are unable to obtain good shape of the J-V curve.

Further, PEDOT:PSS is acidic, corrosive and its properties such as conductivity changes with change of manufacturer. Hence, we were motivated to replace PEDOT:PSS with alternative materials such as- MoO_3, NiO and V_2O_5.

One of the major aspects of designing efficient organic solar cells cells (OSCs) is the engineering of interfacial carrier transport layers between organic layer and metallic electrodes. Among various materials available for interfacial layers, transition metal oxides such as- MoO_3, NiO and V_2O_5, have great potentials owing to the following:

- Wide range of energy level aligning capabilities
- Formation of low resistance ohmic contact by these oxides
- High transparency and desirable band structure
- Excellent ambient stability in ambient environment which can extend the lifetime of organic electronics

The above factors, energy level compatibility (see Figure 5.2), low cost and high throughput production using solution route makes MoO_3 as the most attractive alternative to PEDOT:PSS.

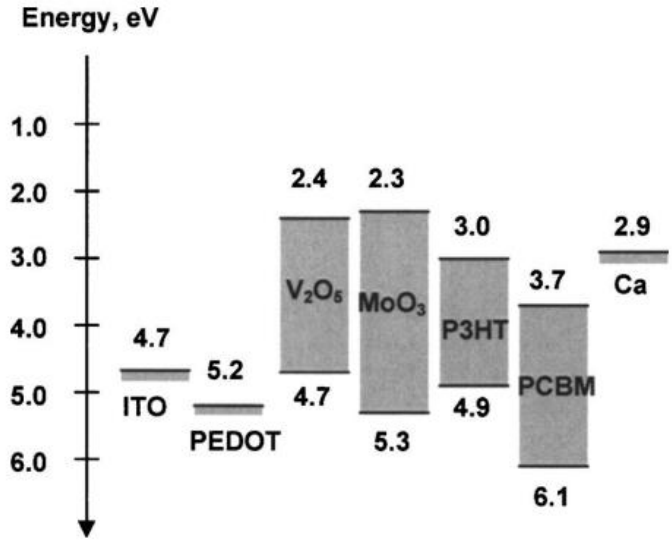

Figure 5.2 Schematic comparing the energy levels of various layers used in OPVs [58]

5.1.2 Replacing PEDOT:PSS with MoO_3 (synthesized through solution route)

The MoO_3 for spin coating is synthesized through solution route. The concentration of the MoO_3 solution used is 2 wt%.

Table 5.2 Device Parameters for device ITO|MoO_3|P3HT:$PC_{60}BM$|Al where MoO_3 is spin coated at 2000 rpm

Fill Factor (FF) **(%)**	**V_{OC}** **(V)**	**J_{SC}** **(mA/cm^2)**	**PCE** **(%)**
32.8	0.51	0.71	0.12

The different parameters of the device ITO|MoO_3|P3HT:PCBM|Al is listed in Table 5.2. These parameters are important in view as this is the first device made in this lab where we have used solution route to make the MoO_3 film. Using this MoO_3 HTL the solar cell showed a fill factor (FF) of 32.8%. The V_{OC} and J_{SC} values were 0.51V and 0.71mA/cm^2 respectively. The power conversion efficiency (PCE) value obtained is 0.12%.

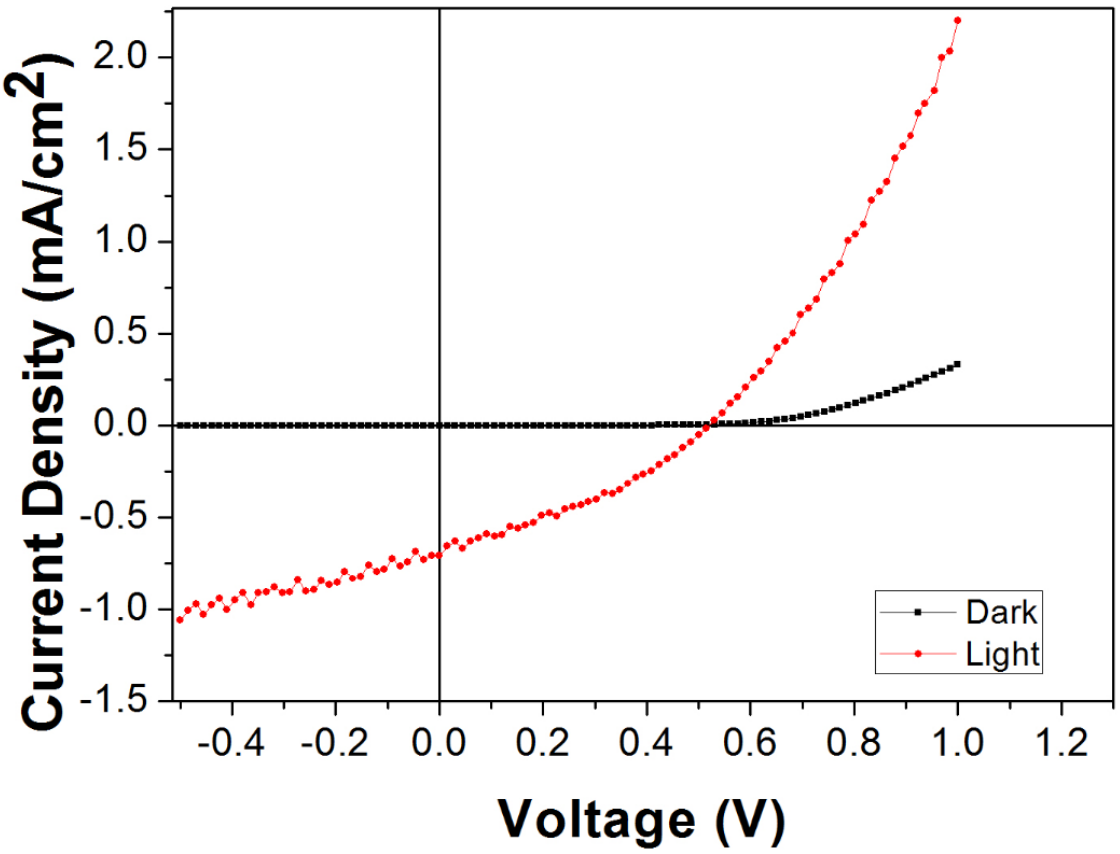

Figure 5.3 J-V plot for solar cell with device structure ITO|MoO_3|P3HT:PC_{60}BM|Al

It is clear from the J-V plot (Figure 5.3) that leakage is present in the solar cell. When MoO_3 is spin coated, MoO_3 nanoparticles may agglomerate and may not give uniform surface morphology. This may increase the roughness of the film which may lead to leakage current. Further AFM study is needed to clarify and establish this concept.

Optimization of MoO_3 film concentration

In view to see the effect of MoO_3 layer thickness on device performance we have tried different concentration of MoO_3 solution (0.2 -2wt%). The J-V plot in light has been shown in Figure 5.4.

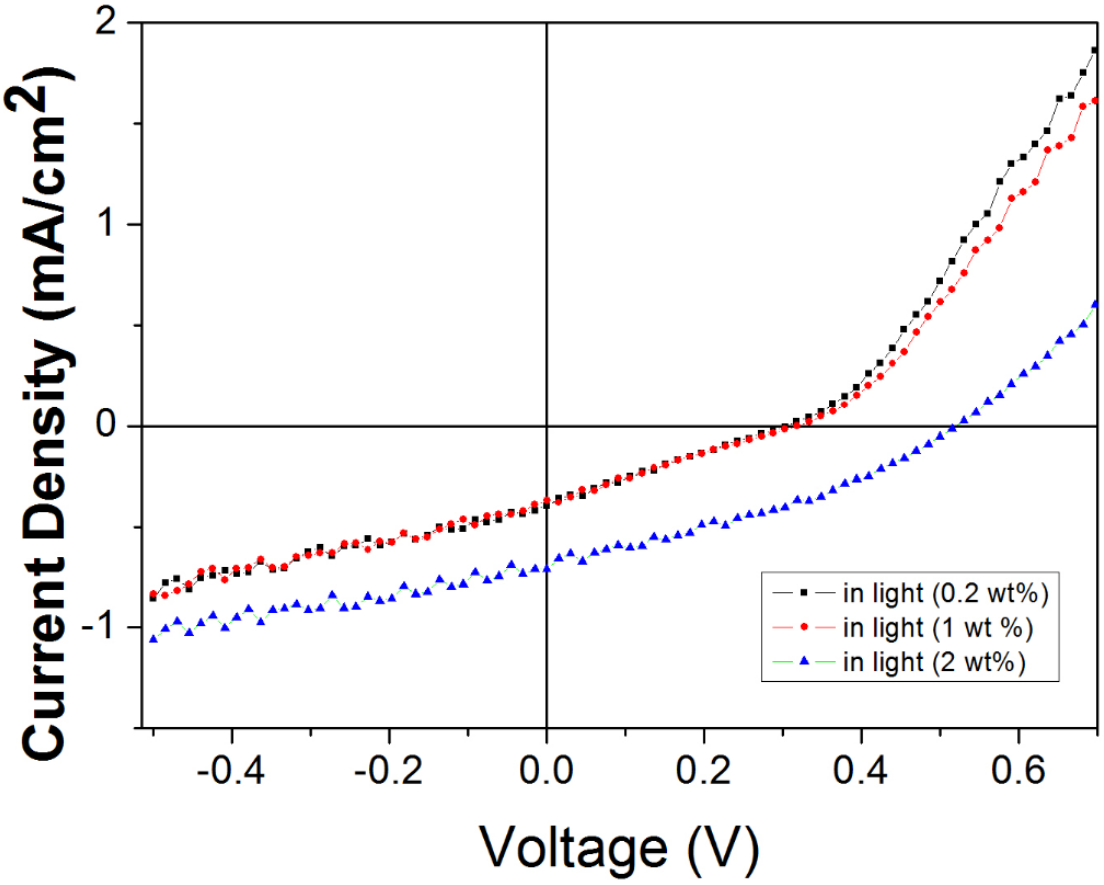

Figure 5.4 J-V plot in light condition for varying concentration of MoO_3 in solar cell with device structure ITO|MoO_3|P3HT:PC_{60}BM|Al

Table 5.3 Device parameters of ITO|MoO_3|P3HT:PC_{60}BM|Al

Concentration (Wt%)	**Fill Factor (FF) (%)**	**V_{OC} (V)**	**J_{SC} (mA/cm^2)**	**PCE (%)**
0.2	23.6	0.30	0.419	0.0030
1	24.6	0.30	0.391	0.0029
2	32.8	0.51	0.71	0.120

It is clear from Table 5.3 that the device ITO|MoO_3|P3HT:PCBM|Al has given the best device parameters for the concentration of 2wt% of MoO_3. In each case the MoO_3 layer has been spin coated at 2000 rpm. As we lower the concentration of MoO_3, the performance of the solar cell decreases. However, still more studies such as AFM are needed to confirm which concentration of MoO_3 gives better film as well as better device performance.

Thus, MoO_3 has the potential to be a good replacement for PEDOT:PSS. Further optimization of the film is required to obtain better device and device efficiency.

Although conventional devices display good performance, these devices degrade at higher rates in air. Extensive investigation of polymer solar cells with an inverted device structure, using modified ITO as cathode is required. These inverted devices are felt to be better as these do not use corrosive PEDOT:PSS and low work function metal cathodes. Further, inverted devices have an advantage of vertical phase separation and concentration gradient in the active layer which shows the self-encapsulating property as air stable materials are used as top electrode. Hence, we were motivated for the study of these inverted devices.

5.2 Study of Inverted Devices:

In case of inverted devices we have used the following general structure:

- ITO|Interface Layer|Active Layer|MoO_3|Al

For our investigation we chose the following device structure:

- ITO|ZnO|P3HT:PCBM|MoO_3|Al

ZnO is good choice because of its environmental stability, relatively high electron mobility and optical transmittance [50] and its wide and direct bandgap (3.37 eV) (Figure 5.5).

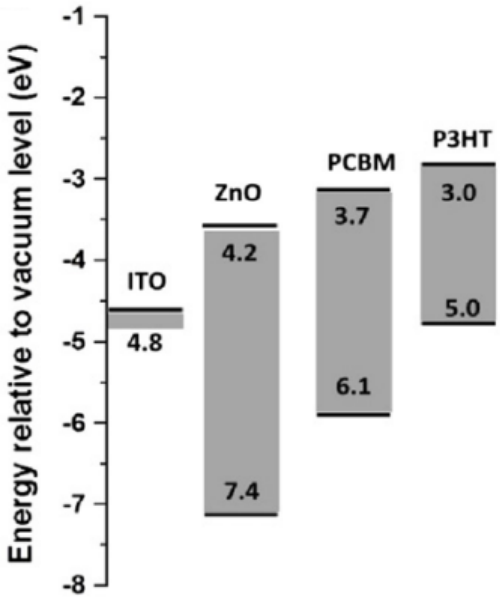

Figure 5.5 Energy level diagram showing ZnO with other materials used [59].

5.2.1 Using ZnO as ETL

ZnO film prepared by solution process is used here. 0.235 g of zinc acetate dihydrate was added in 5 ml propanol and allowed to stir for 5 min. A white cloudy solution is obtained here. Now after 5 minutes, few drops of DEA are added to this solution. Slowly we will observe that the cloudiness disappears and a colourless and transparent solution is obtained. Now, this solution is allowed to stir at 60°C for 2 hours. The solution is then kept untouched and undisturbed for 24 hours. After coating this solution on ITO at 2000 rpm, the substrate should be heated at 200°C for 30 minutes. The active layer tried out with ZnO is P3HT:$PC_{60}BM$.

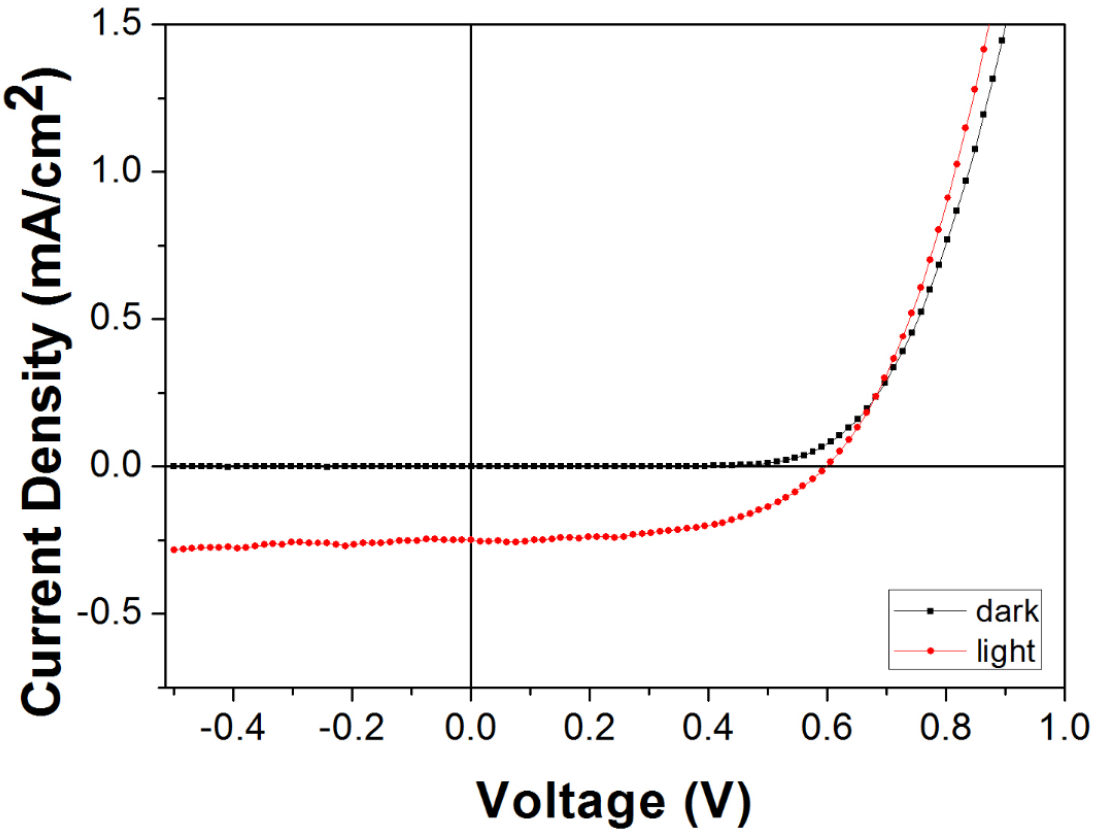

Figure 5.6 J-V plot for solar cell with device structure ITO|ZnO|P3HT:$PC_{60}BM$|MoO_3|Al

Table 5.4 Device parameters for device ITO|ZnO|P3HT:$PC_{60}BM$|MoO_3|Al

Fill Factor (FF) **(%)**	**V_{OC}** **(V)**	**J_{SC}** **(mA/cm^2)**	**PCE** **(%)**
58.2	0.59	0.246	0.084

Good values of fill factor (FF) and open circuit voltage (V_{OC}) were obtained (Figure 5.8). FF obtained was 58.2% and V_{OC} was 0.59V. The short circuit current density (J_{SC}) and power conversion efficiency was 0.246mA/cm^2 and 0.084% respectively.

As seen in Figure 5.6, the solar cell shows almost negligible shunt resistance and excellent fill factor (FF). The only downside is the current density values. They are very

low. We have tried to increase it as mentioned before by using ZnO-polymer composite films as the electron transport layer (ETL). We will see that current density values increase exponentially due to the composite films used. A possible reason for low current density values maybe the defects created in ZnO film during heat treatment and due to the low spatial distribution of ZnO nanoparticles.

Hence, we started thinking about making a composite of ZnO solution with cationic poly-electrolytes and chosen the well-known polymers such as- PSS and PDADMAC.

In pure ZnO film the ZnO nanoclusters have non-homogenous arrangement and no proper connectivity exists between the nanoclusters (Figure 5.7 (a)). On addition of the polymer, the clusters arrange into homogenous manner and the polymer strands bind the clusters together thus providing a suitable connecting path in between the nanoclusters (Figure 5.7 (b)). After addition of the polymer and spin coating it, the film needs to be heated at 200°C for 30 minutes.

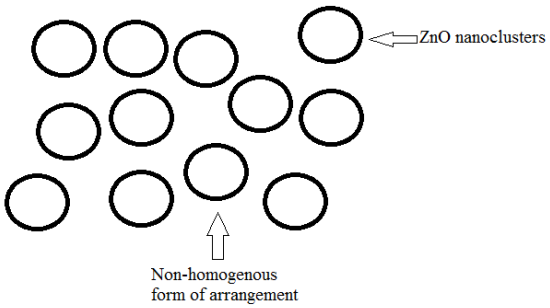

(a)

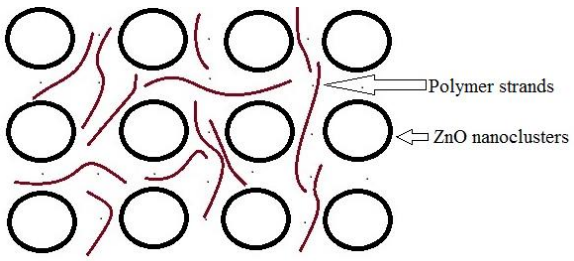

(b)

Figure 5.7 Arrangement of Zno nanoclusters **(a)** before addition of polymer and **(b)** after addition of polymer and heating.

5.2.2 Use of ZnO-PSS nanocomposite

We have tried out another polymer- poly(4-styrenesulfonic acid) (PSS). To make PSS solution we added 0.5 ml PSS in 0.5 ml of water. This solution was stirred for 30 minutes. Now to prepare the nanocomposite solution, this 1 ml PSS solution was added in 2 ml of ZnO solution. Also after a 5 minute interval, 2 to 3 drops of DEA were added in this solution and the resultant mixture was then stirred for 30 minutes.

This ZnO-polymer composite too gives us positive results but with very low current values (Figure 5.8). Further optimization in thickness and concentration is required for this polymer.

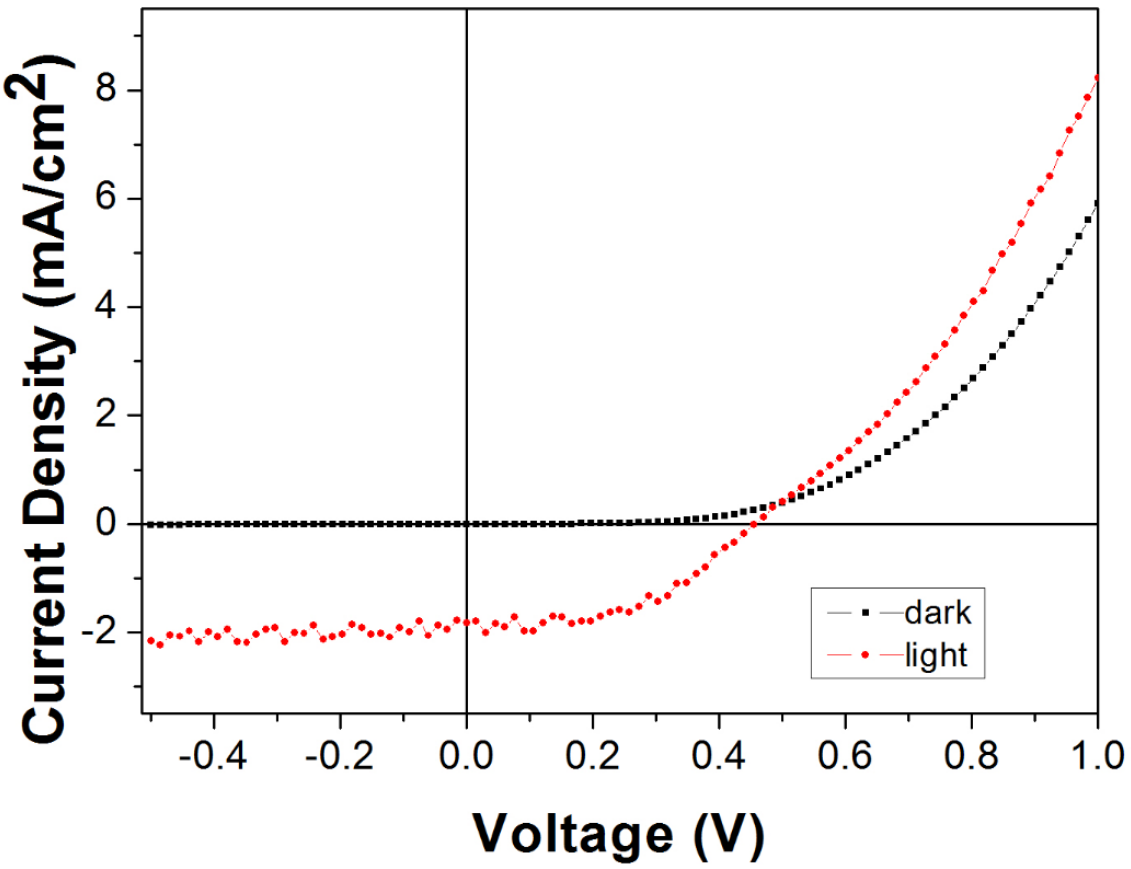

Figure 5.8 J-V plot for solar cell with device structure ITO|ZnO-PSS|P3HT:$PC_{60}BM$|MoO_3|Al

Table 5.5 Device parameters for device ITO|ZnO-PSS|P3HT:PCBM|MoO_3|Al

Fill Factor (FF) (%)	**V_{OC}** (V)	**J_{SC}** (mA/cm^2)	**PCE** (%)
54	0.45	1.77	0.435

The FF and V_{OC} came out to be 54% and 0.45V respectively. The J_{SC} and PCE values are 1.77 mA/cm^2 and 0.435% respectively.

5.2.3 Use of ZnO-PDADMAC nanocomposite layer

This nanocomposite layer was prepared using solution process. To make PDADMAC solution we added 0.5 ml PDADMAC in 0.5 ml of water. This solution was stirred for 30 minutes. Now to prepare the nanocomposite solution, this 1 ml PDADMAC solution was added in 2 ml of ZnO solution. Also after a 5 minute interval, 2 to 3 drops of DEA were added in this solution and the resultant mixture was then stirred for 30 minutes.

PDADMAC is a cationic polyelectrolyte [60] which is widely used as a model for charged polymers behaviour and also in various industrial applications [61,62]. Using this polymer gave us positive results (Figure 5.9).

Using active layer- P3HT:PC_{60}BM:

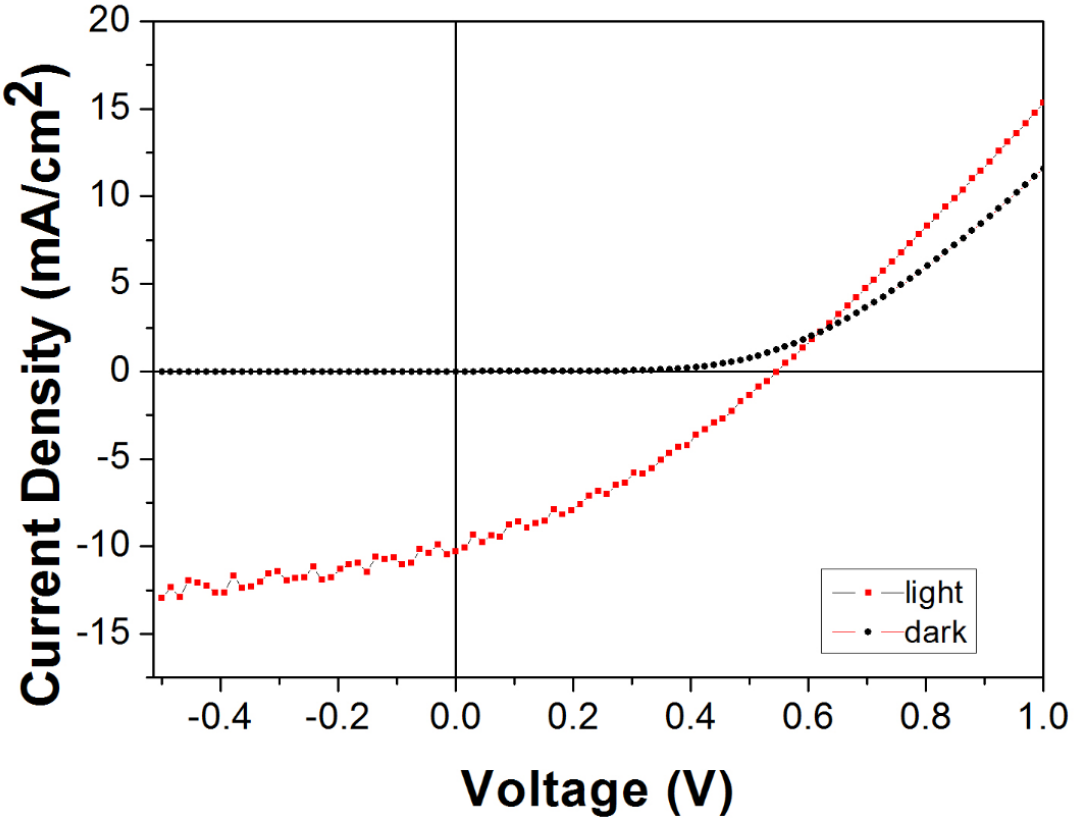

Figure 5.9 J-V plot for for solar cell with device structure ITO|ZnO-PDADMAC|P3HT:$PC_{60}BM$|MoO_3|Al

Table 5.6 Device parameters for device ITO|ZnO-PDADMAC|P3HT:$PC_{60}BM$|MoO_3|Al

Fill Factor (FF) (%)	**V_{OC}** (V)	**J_{SC}** (mA/cm^2)	**PCE** (%)
32.7	0.54	10.82	1.86

Here we obtained high PCE of 1.86% and J_{SC} equal to 10.2mA/cm^2. The V_{OC} and FF values are 0.54V and 32.7% respectively.

Using Active Layer- PCDTBT:$PC_{71}BM$

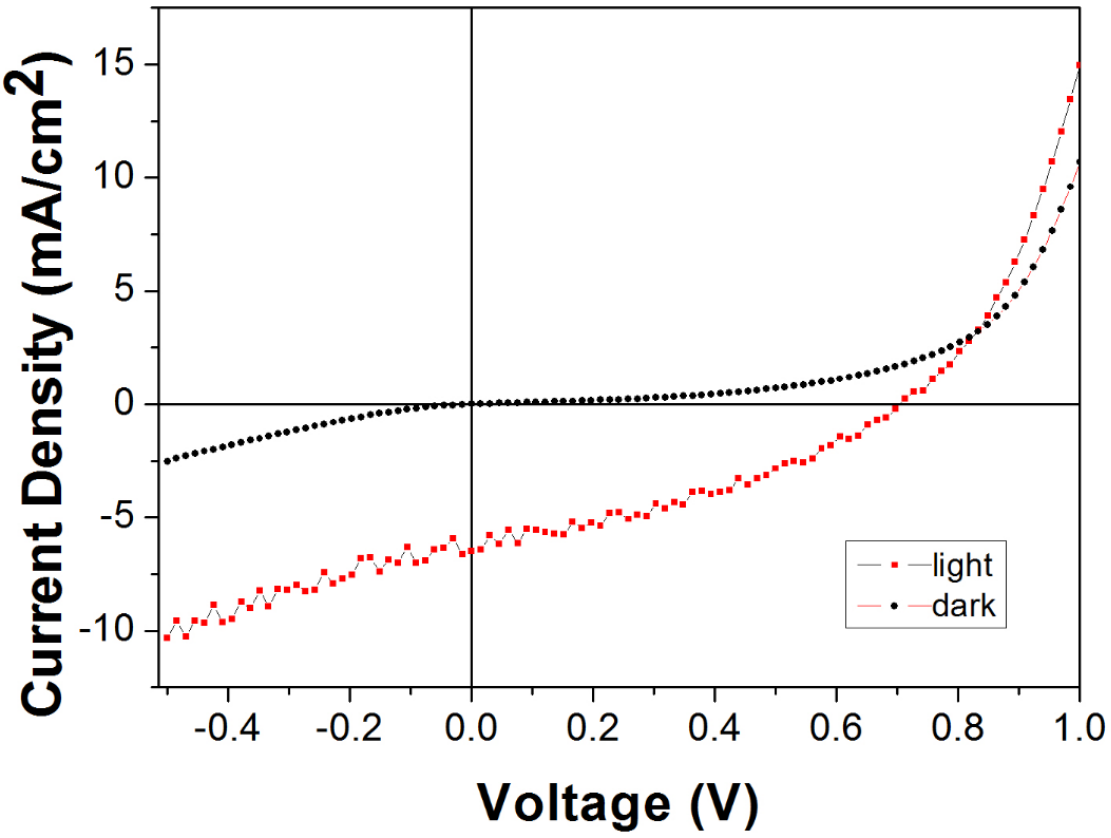

Figure 5.10 J-V plot for solar cell with device structure ITO|ZnO-PDADMAC|PCDTBT:$PC_{71}BM$|MoO_3|Al

Table 5.7 Device parameters for device ITO|ZnO-PDADMAC|PCDTBT:$PC_{71}BM$|MoO_3|Al

Fill Factor (FF) **(%)**	**V_{OC}** **(V)**	**J_{SC}** **(mA/cm^2)**	**PCE** **(%)**
35.2	0.69	6.61	1.62

The PCE of this cell came out to be 1.62% with a V_{OC} of 0.697V. The FF and J_{SC} values were 35.2% and 6.61mA/cm^2 respectively. Seeing these values we can make out that our ZnO-PDADMAC composite layer acts as a successful electron transporting layer (ETL). As observed in Figure 5.10, when active layer- PCDTBT:$PC_{71}BM$ is used, the diode starts showing leakage. This may be due to the incompatibility of the polymer

nanocomposite and the active layer. The presence of defects (such as pin-holes) in the active layer may also give rise to such leakage. Further experiments still need to be carried out to verify this theory.

Change in performance due to variation in light intensity for ZnO-PDADMAC based cell

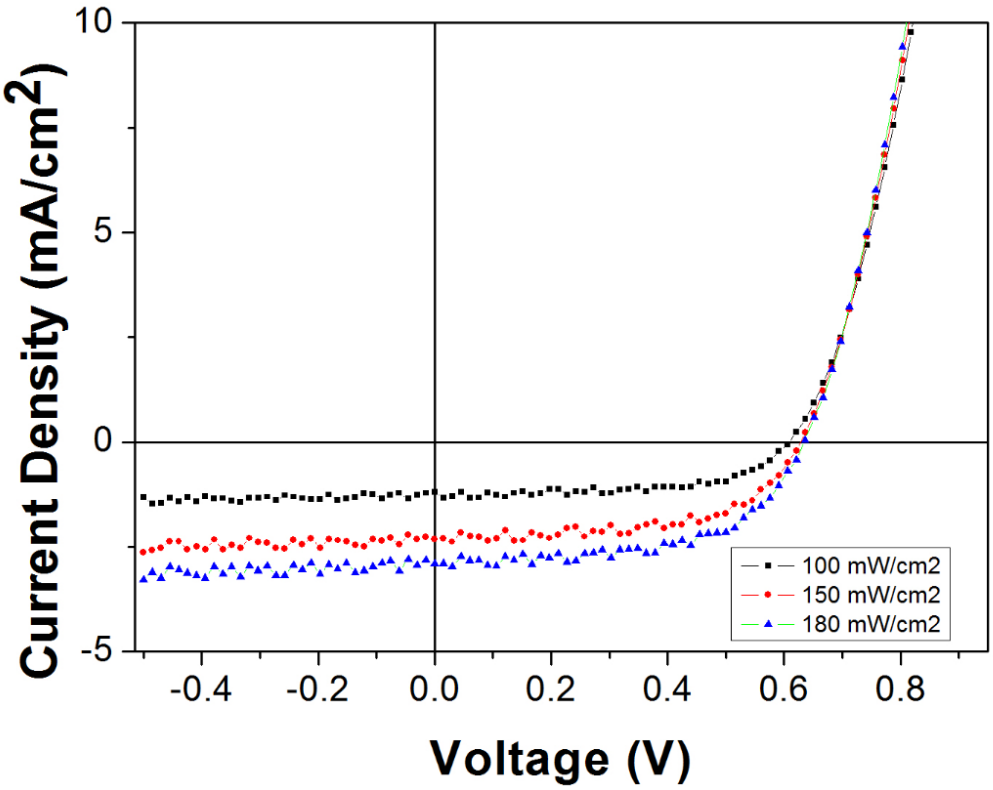

Figure 5.11 Effect of varying the light intensity in J-V plot for solar cell with device structure ITO|ZnO-PDADMAC|P3HT:$PC_{60}BM$|MoO_3|Al

Table 5.8 Device parameters for solar cell with device structure ITO|ZnO-PDADMAC|P3HT:$PC_{60}BM$|MoO_3|Al for different light intensity

Light Intensity (mW/cm^2)	**J_{SC} (mA/cm^2)**	**V_{OC} (V)**	**FF (%)**	**PCE (%)**
100	1.22	0.6	63.6	0.47
150	2.26	0.6	62.1	0.87
180	2.82	0.62	61.3	1.07

As seen in Figure 5.11 and Table 5.8 there is significant effect of varying the light intensity on the performance of the solar cell device. As we increase the light intensity from 100 to 180mW/cm^2, the J_{SC}, V_{OC} and PCE values keep on increasing steadily. On the other hand, the FF value decreases as we increase the intensity. For this observation the active layer (P3HT:$PC_{60}BM$) was annealed in glove box at 120°C for 10 minutes. Due to non-optimized MoO_3 layer, the current values and hence the PCE of the device dropped.

As we have tried different materials as well as different device structures (conventional and inverted) to get rid of PEDOT:PSS, we came to a conclusion that inverted structures using oxides are better alternatives and more focus should be given to these structures.

Chapter 6

Key Achievements

In our investigation of organic solar cell we studied both conventional as well as inverted devices. The device structures investigated here are

(1) ITO|PEDOT:PSS|P3HT:$PC_{60}BM$|Al

(2) ITO|MoO_3|P3HT:$PC_{60}BM$|Al

(3) ITO|ZnO|P3HT:$PC_{60}BM$|MoO_3|Al

(4) ITO|ZnO-PSS|P3HT:$PC_{60}BM$|MoO_3|Al

(5) ITO|ZnO-PDADMAC|P3HT:$PC_{60}BM$|MoO_3|Al

The devices (1) and (2) are simple conventional structures and (3), (4) and (5) are inverted where ITO works as cathode. We have summarized the device parameters in Table 6.1 and 6.2 and their J-V plots in Figure 6.1-6.2.

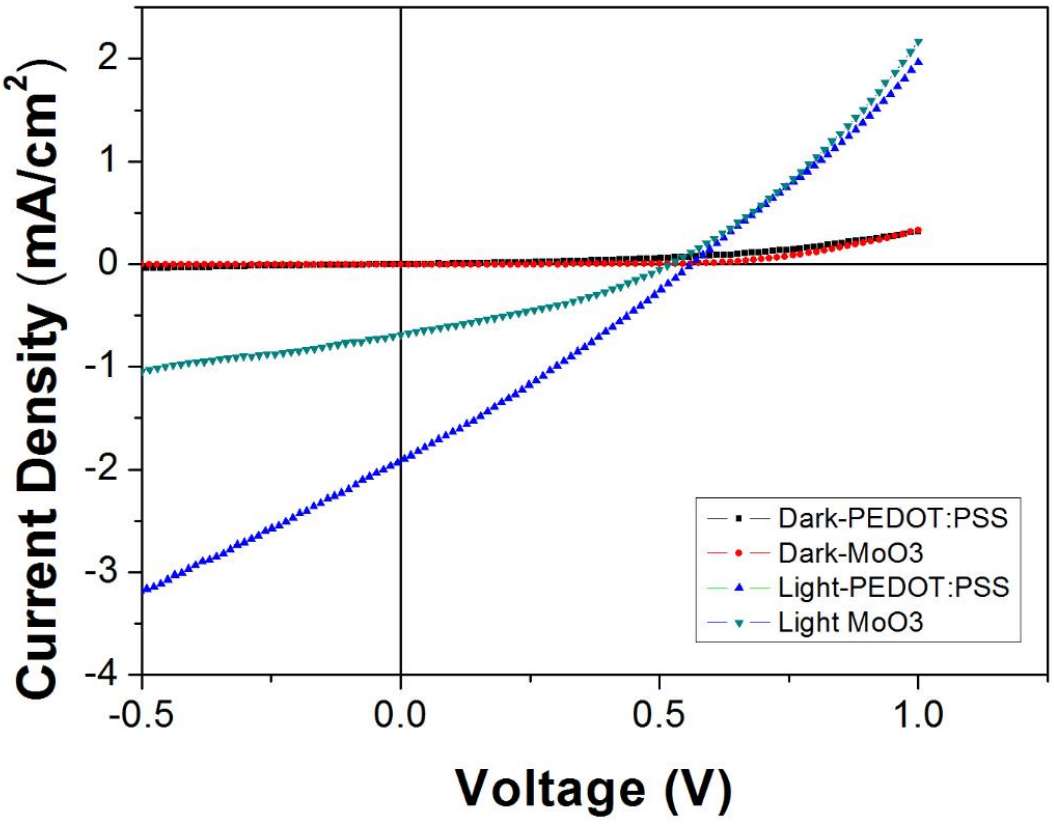

Figure 6.1 J-V plot for devices – ITO|PEDOT:PSS|P3HT:$PC_{60}BM$|Al and ITO|MoO_3|P3HT:$PC_{60}BM$|Al

Table 6.1 Device parameters for the conventional devices- ITO|PEDOT:PSS|P3HT:$PC_{60}BM$|Al and ITO|MoO_3|P3HT:$PC_{60}BM$|Al

Interlayer	**Fill Factor (FF) (%)**	**V_{OC} (V)**	**J_{SC} (mA/cm^2)**	**PCE (%)**
PEDOT:PSS (1500 rpm)	28	0.557	1.97	0.308
MoO_3 (2000 rpm)	32.8	0.51	0.71	0.120

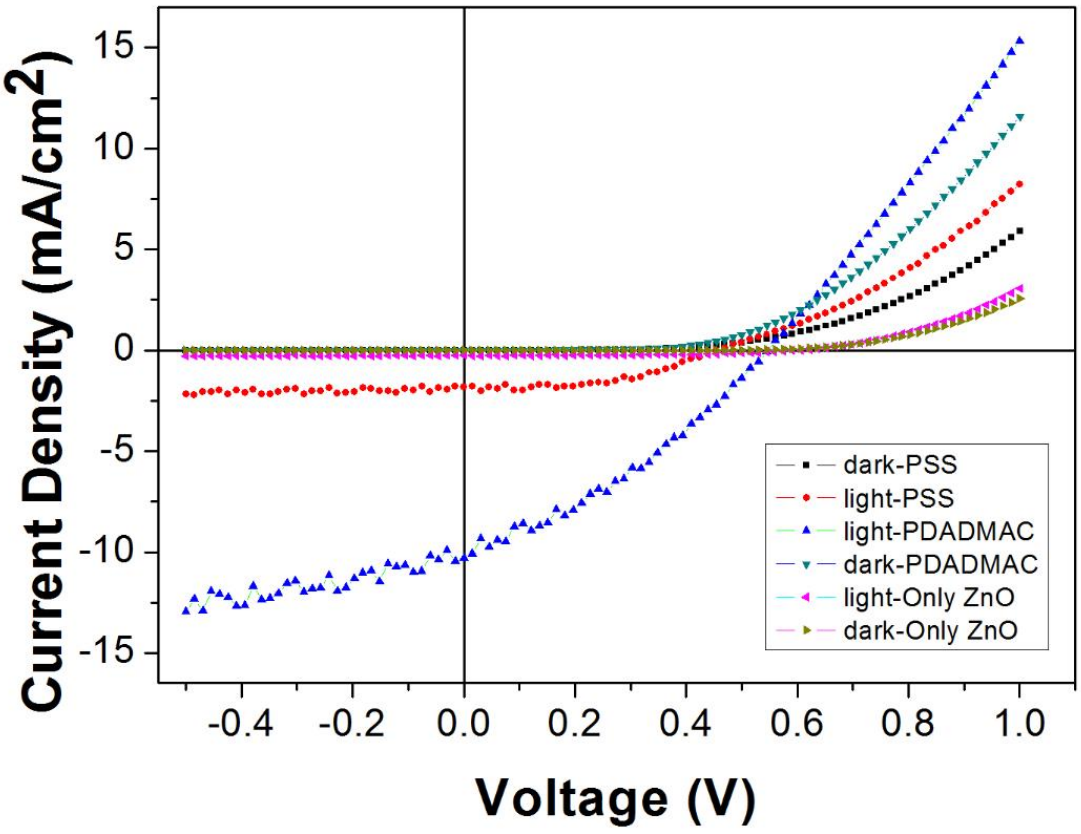

Figure 6.2 J-V plot for devices - ITO|ZnO|P3HT:$PC_{60}BM$|MoO_3|Al, ITO|ZnO-PSS|P3HT:$PC_{60}BM$|MoO_3|Al, ITO|ZnO-PDADMAC|P3HT:$PC_{60}BM$|MoO_3|Al

Table 6.2 Different parameters for inverted devices- ITO|ZnO|P3HT:$PC_{60}BM$|MoO_3|Al, ITO|ZnO-PSS|P3HT:$PC_{60}BM$|MoO_3|Al, ITO|ZnO-PDADMAC|P3HT:$PC_{60}BM$|MoO_3|Al

Interlayer	**Fill Factor (FF) (%)**	**V_{OC} (V)**	**J_{SC} (mA/cm^2)**	**PCE (%)**
ZnO	58.2	0.59	0.246	0.084
ZnO-PSS	54	0.45	1.77	0.435
ZnO-PDADMAC	32.7	0.54	10.82	1.86

Figure 6.1 shows the current density (J) vs. Voltage (V) curves of the conventional devices measured under AM1.5G solar irradiation. In these conventional devices, we demonstrated that an efficient organic solar cell can be fabricated using solution processed molybdenum oxide as an anode interfacial buffer layer. The J-V characteristic curve using solution processed MoO_3 as an anode buffer layer shows a better shape in comparison to PEDOT: PSS. However, further investigations are necessary for these devices in view of leakage current and stability concerns. The devices designed using solution processed MoO_3 may have leakage due to the formation of islands of big agglomerated MoO_3 particles during spin coating and hence morphological investigations of MoO_3 films through AFM may be of very much importance for further optimization studies of the devices.

Again the Figure 6.2 shows the current density (J) vs. Voltage (V) of the inverted devices of design mentioned above as (3) to (5) under AM 1.5 G solar irradiation at an intensity of 100 mW/cm^2. In the ZnO-only devices a typical open circuit voltage (V_{OC}) of 0.59V, short circuit current (J_{SC}) of 0.246 mA/cm^2 and fill factor of 58.2% (see Table 6.2) achieved giving a PCE of 0.084%. When PSS and PDADMAC was added to ZnO to obtain the nanocomposite layer, then the device exhibited improved performance with V_{OC}, $J_{SC,}$ fill factor and PCE of 0.45V, 1.77 mA/cm^2, 54%, 0.435% and 0.54V, 10.82mA/cm^2, 32.7%, 1.86% respectively (see Table 6.2). These device parameters showed superior interface properties of the ZnO-

PSS and ZnO-PDADMAC nanocomposite. The improved electron collection capability of the ZnO-PDADMAC and ZnO-PSS nanocomposite may have resulted in better device parameters (Table 6.2). However, further scrutiny of the electrical characteristics of the ZnO-PSS and ZnO-PDADMAC inter layer in inverted devices is necessary to identify the origin of leakage current. Moreover, as we stated earlier for conventional devices that study of surface morphology of the films is necessary, here also in the case of nanocomposite films it is of very much of importance to study the Zno-PSS and ZnO-PDADMAC film morphology through AFM in order to investigate the reasons behind the leakage current. Probably, the addition of PSS and PDADMAC to ZnO solution works as an excellent surface smoothening material for ZnO planarization. This function may be similar to that of PEDOT:PSS smoothening ITO surfaces and reducing leakage current. Hence this kind of nanocomposite buffer layer may be used to improve the device parameters.

Briefly, we have demonstrated an efficient organic solar cell device by incorporating a solution route synthesized MoO_3 in conventional devices and anode buffer layer, ZnO-PDADMAC and ZnO-PSS nano composite in inverted devices as an electron transport layer. The PSS and PDADMAC not only improved the electron collection efficiency of the inverted devices but also smoothened the ZnO-surfaces, thereby reducing the leakage current and improving the device efficiency. The power conversion efficiency value of 1.86% (see Fig 6.2 and Table 6.2) of a ZnO-PDADMAC nano composite based inverted device is ~22 times higher than that of the device using ZnO as a buffer layer for P3HT: PCBM based system. Further, these inverted devices may show superior air stability and need further investigation. In this way our study represents an alternative approach for developing high–performance organic solar cells.

Chapter 7

Conclusion

The improved electron collection capability of the ZnO-PDADMAC and ZnO-PSS nanocomposite have resulted in better device parameters (Table 6.2). However, further scrutiny of the electrical characteristics of the ZnO-PSS and ZnO-PDADMAC inter layer in inverted devices is necessary to identify the origin of leakage current (as shown in Figure 6.2). Like in conventional devices the examination of surface morphology is necessary ZnO-PSS and ZnO-PDADMAC film morphology through AFM in order to investigate the reasons behind the leakage current. Probably, the addition of PSS and PDADMAC to ZnO solution works as an excellent surface smoothening material for ZnO planarization. This function may be similar to that of PEDOT:PSS smoothening ITO surfaces and reducing leakage current. Hence this kind of nanocomposite buffer layer may be used to improve the device parameters.

Briefly, we have demonstrated an efficient organic solar cell device by incorporating a solution route synthesized MoO_3 in conventional devices and anode buffer layer, ZnO-PDADMAC and ZnO-PSS nano composite in inverted devices as an electron transport layer. The PSS and PDADMAC not only improved the electron collection efficiency of the inverted devices but also smoothened the ZnO-surfaces, thereby reducing the leakage current and improving the device efficiency. The power conversion efficiency value of 1.86% (see Fig 6.2 and Table 6.2) of a ZnO-PDADMAC nano composite based inverted device is ~22 times higher than that of the device using ZnO as a buffer layer for P3HT: PCBM based system. Further, these inverted devices may show superior air stability and need further investigation. In this way our study represents an alternative approach for developing high–performance organic solar cells.

References

1. Data from *U.S. Energy Information Administration*, **2011.**
2. Justin Gillis, Heat-Trapping Gas Passes Milestone, Raising Fears, 28 May **2013**, *The New York Times*.
3. Halls, J. J. M., Cornil, J. dos Santos, D. A., Silbey, R., Hwang, D. H., Holmes, A. B., Brédas, J. L. & Friend, R. H., Charge- and energy-transfer processes at Polymer/polymer interfaces: A joint experimental and theoretical study. *Physical Review B*, **1999**, 60, 5721.
4. Frederik C. Krebs. Polymeric Solar Cells: Materials, Design, Manufacture. DEStech Publications, Inc., Lancaster, Pennsylvania, **2010**.
5. William Shockley and Hans J. Queisser. Detailed balance limit of effeciency of p-n junction solar cells. *Journal of Applied Physics*, **1961**, 32, 510.
6. M. J. Kerr, A. Cuevas, and P. Campbell, Limiting efficiency of crystalline silicon solar cells due to coulomb-enhanced auger recombination, *Progress in Photovoltaics: Research and Applications*, **2003**, 11, 97.
7. M. A. Green, K. Emery, Y. Hishikawa, and W. Warta. Solar cell effeciency tables (version 36). *Progress in Photovoltaics: Research and Applications*, **2010**, 18, 346.
8. Solarbuzz. September URL:http://www.solarbuzz.com/index.asp, **2010**.
9. S. E. Shaheen, D. S. Ginley, and G. E. Jabbour. Organic-based photovoltaics: towards low cost power generation. *MRS Bulletin*, January **2006**, 30, 10.
10. M. LoCascio. Application of semiconductor nanocrystals to photovoltaic energy conversion devices. Evident Technologies, Troy, NY, **2002** (August).
11. M. A. Green, K. Emery, Y. Hishikawa, and W. Warta, Solar cell efficiency tables (version 36), *Progress in Photovoltaics: Research and Applications*, **2010**, 18, 346.
12. Zhicai He, Chengmei Zhong, Shijian Su, Miao Xu, Hongbin Wu and Yong Cao, *Nature Photonics*, **2012**, 6, 591.
13. Lawrence Kazmersk. Best research solar cells effeciencies. NREL, **2010**.
14. R.Gaudiana, C.J.Brabec, Organic materials-fantastic plastic, *Nature Photonics*, **2008**, 2, 287.

15. Tang, C. W. Multilayer organic photovoltaic elements, *US patent 4*, **1979**, 164, 431.
16. Tang, C. W. 2-layer organic photovoltaic cell, *Appl. Phys. Lett.*, **1986**, 48, 183.
17. Gang Li, Rui Zhu and Yang Yang, Polymer solar cells, *Nature Photonics*, **2012**, 6, 153.
18. Yu, G., Gao, J., Hummelen, J. C., Wudl, F. & Heeger, A. J. Polymer photovoltaic cells — enhanced efficiencies via a network of internal donor–acceptor heterojunctions, *Science*, **1995**, 270, 1789.
19. Halls, J. J. M. et al. Efficient photodiodes from interpenetrating polymer networks. *Nature*, **1995**, 376, 498.
20. Gang Li, Rui Zhu and Yang Yang, Polymer solar cells, *Nature Photonics*, **2012**, 6, 153.
21. Li, G. et al. High-efficiency solution processable polymer photovoltaic cells by self-organization of polymer blends, *Nature Mater.*, **2005**, 4, 864.
22. Ma, W. L., Yang, C. Y., Gong, X., Lee, K. & Heeger, A. J. Thermally stable, efficient polymer solar cells with nanoscale control of the interpenetrating network morphology, *Adv. Funct. Mater.*, **2005**, 15, 1617.
23. Richard R. Lunt, Noel C. Giebink, Anna A. Belak, Jay B. Benziger, and Stephen R. Forrest, Exciton diffusion lengths of organic semiconductor thin films measured by spectrally resolved photoluminescence quenching, *Jol. Of Applied Physics*, **2009**, 105, 053711.
24. Introduction to polymer solar cells, René Janssen, Departments of Chemical Engineering & Chemistry and Applied Physics Eindhoven University of Technology, The Netherlands.
25. G. Yu, J. Gao, J.C. Hummelen, F.Wudl, and A.J. Heeger. Polymer photovoltaic cells{ enhanced effeciencies via a network of internal donor-acceptor heterojunctions. *Science*, **1995**, 270, 1789.
26. Frederik C. Krebs. Polymeric Solar Cells: Materials, Design, Manufacture. DEStech Publications, Inc., Lancaster, Pennsylvania, **2010**.
27. Lewis Gomez De Arco, Yi Zhang, Cody W. Schlenker, Koungmin Ryu, Mark E. Thompson, and Chongwu Zhou. Continuous, highly exible, and transparent graphene films by chemical vapor deposition for organic photovoltaics. *ACS Nano*, **2010**, 4(5), 2865.

28. Vipul Singh, Anil K. Thakur, Shyam S. Pandey, Wataru Takashima, and Keiichi Kaneto. A comparative study of al and lif:al interfaces with poly (3-hexylthiophene) using bias dependent photoluminescence technique. Organic Electronics, **2007**, 9(5), 790.
29. M. Girtan and M. Rusu, Role of ito and pedot:pss in stability/degradation of polymer:fullerene bulk heterojunctions solar cells. *Solar Energy Materials and Solar Cells*, **2010**, 94(3), 446.
30. Jiao Li, Juncheng Liu, Congjie Gao, Jinling Zhang, and Hanbin Sun. Influence of mwcnts doping on the structure and properties of PEDOT:PSS films. *International Journal of Photoenergy*, **2009**, article ID-650509.
31. Frederik C. Krebs. Polymeric Solar Cells: Materials, Design, Manufacture. DEStech Publications, Inc., Lancaster, Pennsylvania, **2010**.
32. S. Sista, M.-Hyae Park, Ziruo Hong, Yue Wu, Jianhui Hou, Wei Lek Kwan, Gang Li, and Y. Yang, Highly Efficient Tandem Polymer Photovoltaic Cells, *Adv. Mater*., **2010**, 22, 380.
33. Hao Chen, Linfeng Hu, Xiaosheng Fang, Limin Wu, General Fabrication of Monolayer SnO2 Nanonets for High-Performance Ultraviolet Photodetectors, *Adv. Funct. Mater.*, **2012**, 22, 1229.
34. Kiran Kumar Manga, Junzhong Wang, Ming Lin, Jie Zhang, Milos Nesladek, Venkatram Nalla, Wei Ji, Kian Ping Loh, High-Performance Broadband Photodetector Using Solution-Processible PbSe–TiO2–Graphene Hybrids, *Adv. Mater.*, **2012**, 24, 1697.
35. J. You, Chun-Chao Chen, L. Dou, S. Murase, Hsin-Sheng Duan, S.A. Hawks, T. Xu, H.J. Son, L. Yu, G. Li, Y. Yang, Metal Oxide Nanoparticles as an Electron-Transport Layer in High-Performance and Stable Inverted Polymer Solar Cells, *Adv. Mater*., **2012**, 24, 5267.
36. Huang, F., Wu, H. B. & Cao, Y., Water/alcohol soluble conjugated polymers as highly efficient electron transporting/injection layer in optoelectronic devices, *Chem. Soc. Rev.*, **2010**, 39, 2500.
37. He, Z. et al. Simultaneous enhancement of open-circuit voltage, shortcircuit current density, and fill factor in polymer solar cells. *Adv. Mater.*, **2011**, 23, 4636.
38. National Instruments. Part II - photovoltaic cell i-v characterization theory and labview analysis code, **2012**.

39. PVCDROM website- Solar cell fill factors
40. Jørgensen, M., Bundgaard, E., Bettignies, R.d., and Krebs, F.C., Chapter 2: The Polymer Solar Cell, in Polymer Photovoltaics, A Practical Approach Editor: F.C. Krebs, SPIE - International Society for Optical Engineering, Tech. Univ. of Denmark, **2008**, 11.
41. Dong Hwan Wanga, Jung Kyu Kimd, Jung Hwa Seo, O Ok Parka, Jong Hyeok Park, Stability comparison: A PCDTBT/PC71BM bulk-heterojunction versus a P3HT/PC71BM bulk-heterojunction, *Solar Energy Materials & Solar Cells*, **2012**, 101, 249.
42. R. Schlaf, H. Murata, Z.H. Kafafi, Work function measurements on indium tin oxide Films, *J. Electron Spectrosc. Relat. Phenom*, **2001**, 120, 149.
43. J. Y. Kim, J. H. Jung, D. E. Lee, and J. Joo, *Synth. Met.*, **2002**, 311, 126.
44. J. Hwang, F. Amy, and A. Kahn, *Org. Electron.*, **2006**, 7, 387.
45. H. W. Heuer, R. Wehrmann, and S. Kirchmeyer, *Adv. Funct. Mater.* , **2002**, 12, 89.
46. W. W. Chiu, J. Travaš-Seidić, R. P. Cooney, and G. A. Bowmaker, *Synth. Met.*, **2005**, 155, 80.
47. N. Koch, A. Vollmer, and A. Elschner, *Appl. Phys. Lett.*, **2007**, 90, 043512.
48. Y. J. Lin, H. C. Chang, and B. Y. Liu, *Appl. Phys. Lett.*, **2007**, 90, 112112.
49. Niranjan Sahu, B Parija and S Panigrahi, Fundamental understanding and modeling of spin coating process: A review, *Indian J. Phys*., **2009**, 83 (4), 493.
50. Vacuum generation- rotary vane vacuum pumps, Pfeiffer Vacuum, official website.
51. Kurt J. Lesker and Company. Turbomolecular Pumps and Drag Pumps: Technical Notes.
52. Ensminger Dale, Ultrasonics: data, equations, and their practical uses, CRC Press (Taylor & Francis Group), **2009**, 10. 328.
53. H. K. Lee, J. H. Seo, Y. K. Kim, J. H. Kim, J. R. Koo, K. H. Lee and S. S. Yoon, *J. Korean Phys. Soc.*, **2006**, 49, 1052.
54. E. Aminaka, T. Tsutsui and S. Saito, *J. Appl. Phys.*, **1996**, 79, 8808.
55. S. A. Van Slyke, C. H. Chen, C. W. Tang, *Appl. Phys. Lett.*, **1996**, 69, 2160.
56. J. S. Kim, F. Cacialli, A. Cola, G. Gigli and R. Cingolan, *Appl. Phys. Lett.*, **1999**, 75, 19.

57. Youngkyoo Kim, Amy M. Ballantyneb, Jenny Nelsonb and Donal D.C. Bradley. Effects of thickness and thermal annealing of the PEDOT:PSS layer on the performance of polymer solar cells. *Elseiver, Organic Electronics*, 10, Issue 1, Feb **2009**, 205.
58. Vishal Shrotriya, Gang Li, Yan Yao, Chih-Wei Chu, and Yang Yang, *Appl. Phys. Lett.*, **2006**, 88, 073508.
59. Mohammed Aziz Ibrahema, Hung-Yu Wei, , Meng-Hung Tsai, , Kuo-Chuan Ho, Jing-Jong Shyue, , Chih Wie Chu, Solution-processed zinc oxide nanoparticles as interlayer materials for inverted organic solar cells, *Solar Energy Materials and Solar Cells*, **2013**, 108, 156.
60. Gema Marcelo, M. Pilar Tarazona, Enrique Saiz, *Elsevier Polymer*, **2005**, 46(8), 2584.
61. Dautzenberg H, Go¨rnitz E, Jaeger W., *Macromol Chem Phys* Ed, **1998**,199, 1561.
62. Matsumoto A., *Prog Polymer Science*, **2001**, 26, 189.